Prifysgol Cymru
Y Drindod Dewi Sant
University of Wales
Trinity Saint David

MADE
MANUFACTURE
ADVANCED
DESIGN
ENGINEERING

EXPLORING GENERALISED NEGATIVE INDEX MATERIALS FOR OPTICAL SYSTEMS

JAMES NORMAN MONKS

DRAFT

A DISSERTATION SUBMITTED IN PARTIAL FULFILMENT FOR THE DEGREE OF

MASTER OF SCIENCE

INTERNATIONAL INNOVATION MANAGEMENT

UNIVERSITY OF WALES TRINITY SAINT DAVID

2024

"Every night I lie in bed, the brightest colours fill my head. A million dreams keeping me awake. I think of what the world can be, a vision of the one I see, a million dreams is all it's gonna take. A million dreams for the world we're gonna make"

Ben Pasel & Justin Paul

Name	James Norman Monks	**ID Number**	2126850
Module	Master's Project – Engineering	**Module Code**	ACFA 7003
Supervisor	Alan Mumby	**Date**	
Assignment	Dissertation		
Programme	MSc International Innovation Management	**Word Count**	*

**Excluding dedications, acknowledgements, abstract, preface, content table, titles, captions, figures, tables, equations, references*

DEDICATION

To my beloved daughter – Magi Cêt Monks,

With boundless love and admiration, I dedicate this thesis to you as a beacon of inspiration and limitless potential. May this work stand as a testament to the power of dreams and the significance of embracing the unchartered territories of discovery. May it encourage you to never settle for mediocrity, to seek challenges, and to fearlessly chase after your aspirations, no matter how audacious they may seem.

Embrace your dreams and let them guide you towards a future filled with fulfilment, purpose, and the profound joy of exploring the vast and wondrous unknown.

With all my love.

ACKNOWLEDGMENTS

As I culminate this phase of my academic journey, I feel immense gratitude towards several individuals and groups whose support and guidance have been invaluable.

First and foremost, I extend my heartfelt thanks to my supervisor, Mr. Alan Mumby. His wisdom has been a springboard for my intellectual growth in innovation, providing me with continuous guidance, unwavering support, and ready availability. His encouragement to explore my interests has been a cornerstone for this academic endeavour, for which I am deeply grateful.

I would also like to express my sincere appreciation to the wider academic team. Their support throughout this master's programme has been instrumental in helping me navigate through the challenges and intricacies of the topics discussed.

A special note of thanks goes to my family – my wife and daughter. Their sacrifices and understanding have been the backbone of my journey. The time they have selflessly given up has allowed me to pursue my academic interests and goals. Their patience and love have been a source of constant inspiration and strength. I look forward to getting my weekends and weekday evenings back to spend with these two very special people.

Lastly, I extend my gratitude to the MADE Cymru team. Their goal of providing support and enhancement to the manufacturing sector in Wales has not only impacted numerous lives across this great nation, by also played a pivotal role for me. This unique and fully funded opportunity, supported by the European Union's European Structural and Investment Funds and the Welsh Government, has been a game-changer for many, me included. A deepest thank you to the team for this commitment and vision. May it continue long into the future.

ABSTRACT

PREFACE

Chapter 1 emphasises the progressive innovation of optics and their requirement in modern society from simple mobile phone cameras to surveillance systems; the requirement for increasing complexity while maintaining size, weight, power, and cost is of vital importance. The chapter goes on to discuss the historical scientific development of negative index materials and how a single inspiration paper by Veselago inspired the world for 21st century optical innovation. Moreover, the chapter concludes with arguing the significance of NIMs, their tie to innovation, and a summary of the thesis objectives.

Chapter 2 unravels the background content, and the basic theory and literature associated with optics, such as Maxwell's equations, heavily used in Chapter 4, and aberration theory, explored in Chapter 5.

Chapter 3 presents the methodology of this work including the software used, the design principles, and the limitations of this work.

Chapter 4 explores the mathematical representation for deriving and designing NIMs from first principles through understanding how the electrons within materials interplay and manipulate a materials ability to control the electric and magnetic fields, in order to facilitate time positional resonance that can regulator dispersion within the materials.

Chapter 5 concerns common optical design principles to understand the unique advantages of spherically shaped lenses made from negative indexed material have over conventionally positive indexed materials, showcasing how third-order aberrations are improved with NIM lenses.

Chapter 6 applies the principles developed in Chapters 4 and 5 to an industry 4.0 problem of how automated systems can "see" problems, particularly in three-dimensions without binocular imaging systems.

Chapter 7 concludes the thesis and aims to answer the central question: Do the benefits of incorporating generalised NIM lenses into optical systems through SWAP-C optimisation exist, and if so, how can they drive optical innovation?

TABLE OF CONTENTS

DEDICATION iv

ACKNOWLEDGMENTS v

ABSTRACT vi

PREFACE vii

TABLE OF CONTENTS viii

LIST OF TABLES x

LIST OF FIGURES xi

LIST OF ABBREVIATIONS xiii

1 Introduction: Illuminating the Path 1

1.1 The Driving Force 2

1.2 Historical Context 2

1.3 Ripple Effects: Significance & Impact 13

1.4 Ties to Innovation 13

1.5 Guiding the Reader: Objectives & Thesis Structure 14

2 Background: Unravelling the Light 15

2.1 Optical Innovation 15

2.2 Electromagnetic Theory 16

2.3 Optics 20

3 Methodology: Crafting the Vision 26

3.1 Art, Engineering & Science 26

3.2 Optical Design Process 27

3.3 Selection of Negative Index Glass Materials 29

3.4 Design & Simulations 30

3.5 Limitations 30

4 **Mathematical Characterisation**: Inverting the Spectrum 32

4.1 Birth of Negative Index Glasses 32

4.2 Dispersion Dynamics 41

4.3 Chapter Summary 47

5 **The Fundamentals of NIM Lenses**: Focusing on Refraction 48

5.1 Thin Lens Equation 48

5.2 Thick Lens Equation 52

5.3 Aberration 53

5.4 Chapter Summary 60

6 **Optical Design**: An Industry 4.0 Machine Vision Application 61

6.1 Introduction to Optics in 3D Imaging 61

6.2 Methods for Non-Contact 3D Metrology in I4.0 61

6.3 Challenges in Optical Design for 3D Imaging 62

6.4 Optimisation Techniques 62

6.5 Noteworthy Benefits to the NIM Solution Over the PIM Solution 63

6.6 Optical Solution of Broadband White Light System using NIM Lenses 66

6.8 Chapter Summary 72

7 **Conclusion**: Converging the Future 73

7.1 Conclusion 73

7.3 Suggestions for Future Work 76

REFERENCES 77

LIST OF TABLES

Table 1.1. Example of technology inspired by Victor Veselago's work. 7
Table 2.1. Maxwell's equations. 18
Table 2.2. The five Seidel aberrations..... 24
Table 4.1. Material parameters for calculating the two artificial NIMs presented in *Figure 4.7*. 46
Table 4.2. Properties of the two artificial NIMs. 46
Table 5.1. Table of equations to calculate a defined lens bending according to the focal length and negative refractive index. An example has also been provided. 50
Table 5.2. Comparison of the thin and thick lens when $n = -1.5$ and $d = 2mm$..... 53
Table 5.3. Simplified Siedel aberration equations. 54
Figure 5.7. 3D plots of the primary monochromatic aberrations showing the effects of refractive index and lens curvature combined, with 2D isometric projections highlighting the extremes. 57
Figure 5.8. Ray traced diagrams show the effects of lens shape with positive and negative refractive index. The Seidel aberrations demonstrate the improved comparative performance for negative index lenses. The grid lines are spaced at 0.02mm. aberrations are indicated as spherical (s1), coma (s2), astigmatism (s3), field curvature (s4), and distortion (s5). 59
Table 6.1. Comparison of broadband solution using NIMs compared with the traditional laser triangulation method. 64
Table 6.2. Key advantages for i4.0 applications. 65
Table 6.3. The design prescription of the two designs. 67
Table 6.4. Comparative summary of the aberrations found in both Figure 6.2 designs. 71

LIST OF FIGURES

Figure 1.1. Classification of materials based on the permittivity and permeability. 6
Figure 1.2. Example of calculated invisibility cloaking device. The black dotted line represents the cloak with the central region being invisible to the outside world. 8
Figure 1.3. A 20mm thick plano-plano slab demonstrating the power of NIMs as proposed by Pendry. (a) Positive index of $n = 1$. (b) Negative index of $n = -1$..... 10
Figure 2.1. The discrete breakdown of the electromagnetic spectrum with the visible spectrum highlighted. 17
Figure 2.2. Snell's law of refraction illustrated for an ordinary case (positive index) and an unconventional case (negative index)..... 19
Figure 2.3. Discrete areas of optical physics through time..... 21
Figure 2.4. Demonstration of Ray optics formulated from the perpendicular of the wavefront. 22
Figure 2.5. Example of stigmatic imaging via a tiny aperture with a unity magnification..... 23
Figure 4.1. (a) Neutral particle without an external electric field. (b) Particle displaying dipole properties due to the external electric field..... 33
Figure 4.2. A simplistic representation of interband electron transitions vs intraband electron transitions..... 34
Figure 4.3. The Drude-Lorentz permittivity for a conjectural material with $\omega 0{=}4$, $\omega p{=}5$, and $\gamma{=}0.3$. 37
Figure 4.4. The Drude permittivity for a conjectural material with $\omega p{=}5$, and $\Gamma{=}0.3$. The Plasmas Frequency is the point at which the real part switches from negative to positive..... 38
Figure 4.5. (a) The dispersion variation between three types of glass. (b) Abbe diagram with glass classifications..... 42
Figure 4.6. Example of real parts of the negative refractive index dispersion in visible spectrum, derived from the Drude and Drude-Lorentz model. 45
Figure 4.7. Example of two calculated negative refractive index materials with different dispersion behaviours, derived from the Drude and Drude-Lorentz model. 46
Figure 5.1. Illustration of how a fish is seen by an observer in (*right*) positive index material, and (*left*) negative index material. 49
Figure 5.2. The associated radii for $R1$ and $R2$ for a given lens bending parameter (α), where $f = 50mm$ and $n = -1.5$. 51
Figure 5.3. Comparison example of the lens curve for positive and negative refractive indices ($n = \pm 1.5$) with focal point of $f = 50mm$ and thickness of edge of $1mm$ 52
Figure 5.4. Simulation setup. 54
Figure 5.5. Aberrations for varying refractive index with lens shape factor set to zero (symmetric curvature radii) for set up found in Figure 5.4. The grid lines are spaced at 0.01mm. Spherical (red), come (green), astigmatism (purple), field curvature (blue), and distortion (yellow). 56

Figure 5.6. Ray traced diagrams comparing index variation of ±1.25 with a lens shape factor of zero. The RMS is measured in radians. The spot diagram zooms are shown to the *right*. Lens thickness is 1.5 mm. The field axis is at 4°. 57
Figure 6.1. Schematic demonstrating different object distances that have different image distances. Scheimpflug's idea involves tilting the sensor plane to perceive the depth of focus. 62
Figure 6.2. Optical design of 3D Industry 4.0 imaging system with (a) positive index materials and (b) negative index materials. The ray colours differ to highlight the varying fields, not the wavelength of light. 66
Figure 6.3. A comparative chromatic focal shift evaluation. *Insert* showing the extent of the NIM focal shift. 68
Figure 6.4. Simulated image through the optical systems of (a) positive index design, and (b) negative index design. 69
Figure 6.5. A comparative aberration evaluation of (a) positive index design, and (b) negative index design. 70

LIST OF ABBREVIATIONS

BSU	Boise State University
GC	Graduate College
TDC	Thesis and Dissertation Coordinator
AEAFUIGCTDT	An Example Abbreviation for Use in the Graduate College Thesis and Dissertation Template

[*This page intentionally left blank*]

1

INTRODUCTION: ILLUMINATING THE PATH

In the ever-evolving landscape of optical technologies, the continuous pursuit of cutting-edge advancements and ground-breaking innovations has been the driving force behind the development of state-of-the-art imaging systems. From the humble origins of the camera obscura to the sophisticated devices that permeate our daily lives today, our unyielding quest to capture, analyse, and interpret the visual world around us has been one of the most critical aspects of human innovation. This dissertation seeks to explore the frontier of negative index glass lenses, a ground-breaking theoretical development that promises to revolutionise the way society perceives and interacts with the world through optical devices.

Traditionally, conventional lenses (i.e., positive refractive index materials) have been the backbone of imaging systems. However, they have inherent limitations that hinder their performance in applications demanding high precision, compactness, or ultra-high resolution. These limitation stem from the fundamental properties of conventional materials manifesting themselves as optical aberrations, which degrade image quality and constrain the potential of imaging systems. The creation of negative index materials (NIMs) and their implementation in

glass lenses offers a tantalising glimpse into a world of optical systems unshackled from the restraints of conventional lens design.

1.1 The Driving Force

In today's fast-paced, technologically advanced world, optical imaging and display systems have become an integral part of our daily lives. From consumer cameras to long-range surveillance equipment, advancements in digital sensors and displays have revolutionised numerous applications. In an increasingly competitive market, there is a relentless push to improve optical performance while reducing size, weight, power, and cost – a concept known as SWAP-C.

The quest to improve SWAP-C is often hindered by the limitation of optics themselves. While electronic components have experienced a significant size reduction due to the industries collective drive to continue Moore's law, optical modules are constrained by their fundamental properties. Therefore, strategies to enhance SWAP-C focus on decreasing the number, size, and density of optical components. Innovative technologies like aspheric surfaces and diffractive-refractive hybrid optics demonstrate promising results by reducing mass and cost while maintaining performance.

NIMs present an innovative approach to minimise the SWAP-C of traditional optical systems. By integrating negative properties into an optical component, aberration correction in an optical system can be enhanced without increasing mass. Consequently, this allows for a balance between performance improvement and the reduction of size or optical component-count.

1.2 Historical Context

The refractive index is a fundamental property of material that quantifies the extent to which light is bent, or refracted, as it passes through the material. One of the earliest investigations into the phenomenon of refraction was conducted by Ptolemy in Alexandria, Egypt, around the 2nd

century AD. Ptolemy's work, however, provided an incomplete understanding of refraction and was limited to small angles.

A more accurate description of the relationship between refraction angles was discovered by the Persian scientist Ibn Sahl in 984 AD. Sahl's findings were recorded in his manuscript, "On Burning Mirrors and Lenses," where he used the law refraction to derive lens shapes that focus light. Despite the ground-breaking nature of Sahl's work, the law of refraction would later be named after the Dutch astronomer Willebrord Snellius (Snell), who rediscovered the law in 1621.

The refractive index is intimately related to the permittivity and permeability. In simplistic terms, the permittivity (ε) quantifies a material's ability to transmit electric fields, while permeability (μ) quantifies the material's ability to transmit magnetic fields. The connection between these properties and the refractive index (n) can be expressed as:

$$n = \sqrt{\varepsilon\mu}$$

The relationship was later formulated in the context of James Clerk Maxwell's equations, developed in 1859, which provided a unified description of the electric and magnetic fields and their interactions.

The idea of materials with a negative refractive index emerged in 1967 when Russian physicist Victor Veselago proposed the existence of materials with negative permittivity and negative permeability. According to Veselago's theory, these materials would exhibit a negative refractive index, resulting in unconventional interactions with electromagnetic radiation. At the time, Veselago's idea were purely theoretical, as no naturally occurring materials with a negative refractive index were known.

Interest in NIMs grew in the late 1990s with the exploration of artificial materials, known as metamaterials, which exhibit unique electromagnetic properties. A British theoretical physicist,

John Pendry, contextualised Veselago's work and proposed the concept of a "perfect lens" made from a negative index material. This lens, also known as a *Superlens*, would be capable of overcoming the diffraction limit – a fundamental constraint in conventional optics that limits the resolution of images.

The first experimental demonstration of a negative refractive index material was achieved in 2001 by a team led by David R. Smith at the University of California, San Diego. This metamaterial exhibited a negative index of refraction for microwave frequencies, providing experimental validation for Veselago's theoretical predictions.

Since then, the study of NIMs has gained significant attention due to their potential applications in optics, communications, and other areas of science and technology. Progress in the field has been driven by advancements in nanotechnology and material fabrication techniques, which have enabled the creation of metamaterials with negative refractive indices at higher frequencies, including visible light. Despite the challenges associated with the fabrication and loss characteristics of these materials, the potential for ground-breaking applications continues to inspire researchers worldwide.

Electrodynamics of Medium with Simultaneously Negative Values of ε & μ

Victor Veselago's seminal 1967 paper, *titled the same as this subsection (Russian translated)*, introduced a novel theoretical concept of materials with negative permittivity and permeability. This work laid the groundwork for the study of negative refractive index materials and metamaterials.

Veselago began his analysis by examining the wave equation in a medium with negative ε and μ. The wave equation for an electromagnetics wave propagating in a linear, homogeneous, and isotropic medium can be expressed as:

$$\nabla^2 E = (\varepsilon\mu)\frac{\partial^2 E}{\partial t^2}$$

Where E is the electric field and t is time. In a medium with negative ε and μ, the product (εμ) remains positive, meaning that the wave equation retained its form.

The Russian physicist discovered that in a medium with negative ε and μ, the phase and ground velocities have opposing directions. Mathematically, the phase velocity (v_p) and ground velocity (v_g) can be defined as:

$$v_p = \frac{c}{n}$$

And

$$v_g = \frac{\partial\omega}{\partial k} = c\frac{dn}{d\omega}$$

Where c is the speed of light, n is the refractive index, ω is the angular frequency, and k is the wave number. In a medium with a negative ε and μ, the refractive index is also negative, resulting in a phase velocity opposite to the direction of wave propagation.

Veselago analysed the reflection and refraction of electromagnetic waves at the interface between a normal medium (i.e., with positive ε and μ) and a medium with negative ε and μ. Applying the boundary conditions for the electric and magnetic fields, he derived a modified form of Snell's law.

$$n_1 \sin(\theta_1) = -\, n_2 \sin(-\theta_2)$$

For the case where n_2 is negative, Veselagos analysis revealed that the angle of refraction (θ_2) would be negative. This means that the refracted wave would propagate in the opposite direction of what would be expected for a normal medium.

Veselago also examined the Poynting vector (S), which represents the flow of energy in an electromagnetic wave. Generally, the Poynting vector can be given by:

$$S = \left(\frac{1}{\mu_0}\right) E \times B$$

Where E is the electric field, B is the magnetic flux, and μ_0 is the permeability of free space. Note that $\times$ is the cross product, not a multiplication factor. In a negative medium, E and H reverse their direction, causing the Poynting vector to maintain the same direction as the group velocity. This ensures that energy flow is consistent with the wave propagation direction.

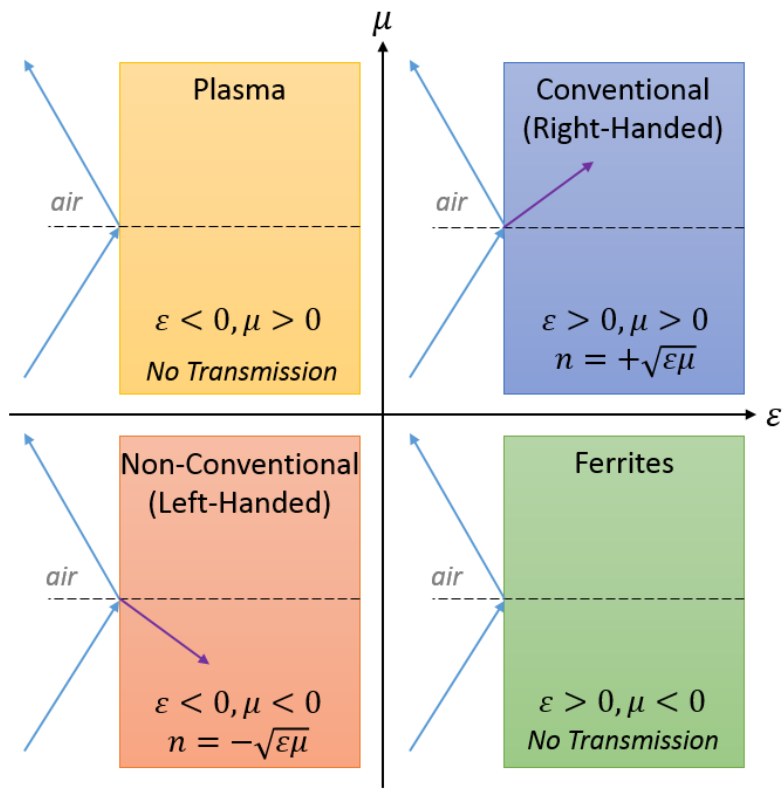

Figure 1.1. Classification of materials based on the permittivity and permeability.

The paper also explored other unconventional properties exhibited by NIM, such as the reversal of the Doppler effect, Cherenkov radiation, and the Goos-Hanchen effect. He found that the Doppler shift in a NIM would have the opposite sign compared to a normal medium, resulting in a “blue shift” when moving away from the source and a “red shift” when moving towards it.

Similarly, Cherenkov radiation in a negative index material would propagate in the opposite direction of the charged particle generating it. These findings further highlighted the unique and counterintuitive behaviour of electromagnetic waves in materials with negative ε and μ.

Victor Veselago's work has inspired decades of research into metamaterial and NIMs, leading to numerous applications and advancements in the field of optics and photonics, including those presented in table 1.

Table 1.1. Example of technology inspired by Victor Veselago's work.

Technology	*Description*
Superlenses	Negative index material can be used to create lenses that surpass the diffraction limit, allowing for imaging and resolution beyond conventional optics.
Invisibility cloaking devices	By manipulating the propagation of electromagnetic waves, NIMs can be used to develop invisibility cloaks that hide objects from detection.
Antennas and Waveguides	The unique properties of negative index materials can be employed to design compact and efficient antennas, as well as waveguides with improved performance.
Enhanced nonlinear optics	The use of NIMs can lead to the enhancement of nonlinear optical effects, enabling the development of novel photonic devices and systems.

The ground-breaking paper provided a theoretical framework for understanding the behaviour of electromagnetic waves in materials with simultaneously negative ε and μ, opening the door for the development of negative index materials and metamaterials.

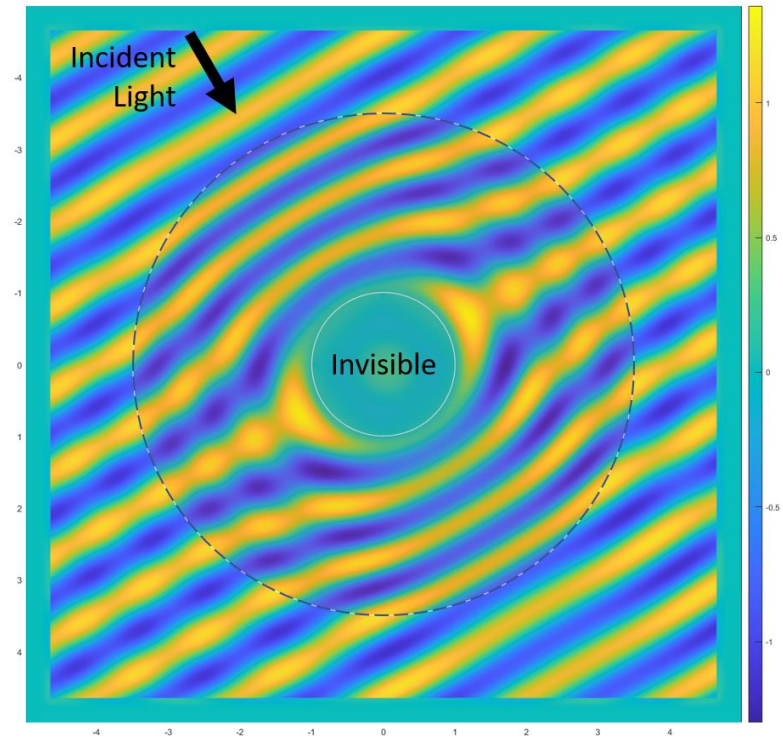

Figure 1.2. Example of calculated invisibility cloaking device. The black dotted line represents the cloak with the central region being invisible to the outside world.

THE PERFECT LENS

John Pendry's influential 2000 paper, "Negative refraction makes a perfect lens," built upon Veselago's theoretical foundation to propose a lens capable of achieving perfect imaging resolution, beyond the diffraction limit. This *perfect lens* utilises NIMs to enable extraordinary optical properties.

The resolution of conventional lenses is limited by the diffraction of light, which imposes a fundamental limit on the smallest resolvable features. The diffraction limit is defined by the Abbe criterion:

$$\Delta x \approx \frac{\lambda}{2NA}$$

Where Δx is the minimum resolvable distance, λ is the wavelength of light, and NA is the numerical aperture of the lens.

Pendry proposed that a lens made from a negative index material can overcome the diffraction limit by capturing and focusing evanescent waves, which contain high spatial frequency information typically lost in conventional imaging systems. A perfect lens would exhibit a negative refractive index of $n = -1$, enabling the lens to focus both propagating and evanescent waves.

The basis of Pendry's perfect lens theory lies in the wave vector (k) components. In a conventional lens, the transverse wave vector component ($k_\perp$) is conserved, while the longitudinal component ($k_\parallel$) is lost due to evanescent wave decay. In a NIM, however, both components can be conserved, allowing for the transmission of subwavelength details. The relationship between the wave vector component in a NIM with $n = -1$ is given by:

$$k'_\perp = -k_\perp$$

$$k'_\parallel = k_\parallel$$

Where $k'_\perp$ and $k'_\parallel$ are the wave vector components in the NIM.

In his paper, Pendry demonstrated that a slab of negative index material with $n = -1$ would form an image on the opposite side of the slab at a distance equal to the object's distance from the slab. The resulting image would have a one-to-one correspondence with the object, enabling perfect imaging resolution.

While Pendry's perfect lens theory provides a compelling concept for surpassing the diffraction limit, several practical challenges must be addressed in the realisation of such a lens.

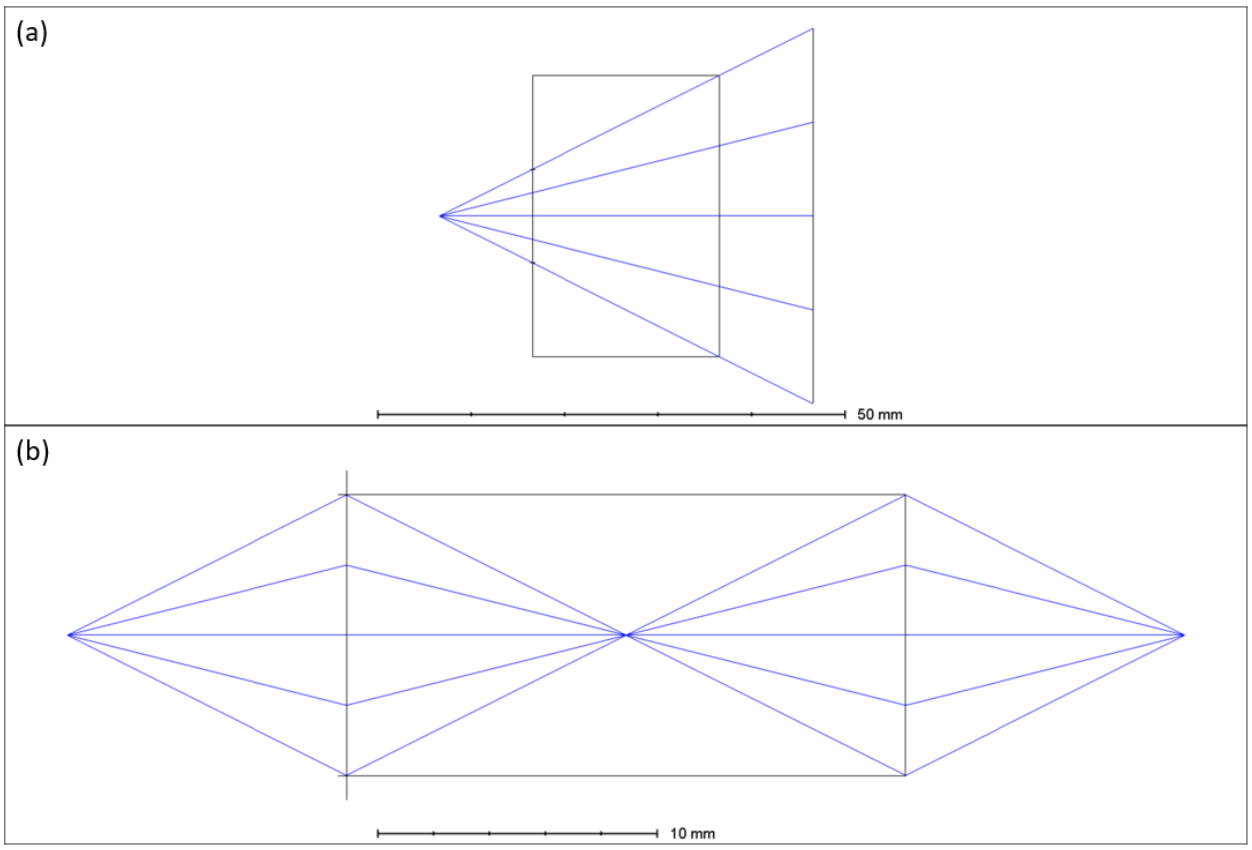

Figure 1.3. A 20mm thick plano-plano slab demonstrating the power of NIMs as proposed by Pendry. (a) Positive index of $n = 1$. (b) Negative index of $n = -1$.

This radical paper on the perfect lens has provided new insights into the potential applications of NIMs and has spurred significant research in the fields of optics and photonics. By proposing a lens capable of surpassing the diffraction limit, Pendry opened the door to a new era of optical science discovery.

The Birth of Metamaterials

The work presented by Veselago and Pendry provided the footprints for metamaterials. The concept further emerged from a pioneering fusion of material science, electromagnetism, and optics, as researchers sought to engineer artificial materials with extraordinary properties not found in nature.

Metamaterials are synthetic materials with tailored properties that arise from their engineered structure rather than their chemical composition. These artificial materials can manipulate electromagnetic waves in unconventional ways, leading to unique phenomena such as negative refraction, invisibility cloaking, and super-resolution imaging.

Metamaterials are typically composed of subwavelength structures known as meta-atoms, which are often designed as periodic arrangements of electric and magnetic resonators. The interactions between these resonators and incident electromagnetic waves determines the effective permittivity and permeability of the metamaterial. The effect medium approximation, namely the Maxwell Garnett equation, can be used to describe the bulk properties of metamaterials:

$$\left(\frac{\varepsilon_{eff} - \varepsilon_m}{\varepsilon_{eff} + 2\varepsilon_m}\right) = f_i \left(\frac{\varepsilon_i - \varepsilon_m}{\varepsilon_i + 2\varepsilon_m}\right)$$

$$\left(\frac{\mu_{eff} - \mu_m}{\mu_{eff} + 2\mu_m}\right) = f_i \left(\frac{\mu_i - \mu_m}{\mu_i + 2\mu_m}\right)$$

Where ε_{eff} and μ_{eff} are the effective permittivity and permeability respectively, f_i is the volume fraction of the *ith* constituent, ε_m and μ_m are the host medium properties, and ε_i and μ_i are the *ith* constituent properties.

The early development of metamaterials focused on the engineering of structures that exhibited negative permittivity and permeability, as inspired by Veselago's theoretical work. In 1999, Pendry et al., proposed the split-ring resonator (SRR) as a magnetic resonator capable of achieving negative permeability at microwave frequencies. SRRs consist of concentric metal rings with gaps that generate magnetic resonance in response to an incident magnetic field. In parallel, wire medium structures were developed to achieve negative permittivity. Wire medium consists of parallel metallic wires that respond strongly to incident electric fields, leading to a plasma-like behaviour at specific frequencies.

The combination of SRRs and wire medium enabled the design of the first negative index metamaterial, demonstrated experimentally by Smith et al. in 2000. Their work provided experimental evidence of negative refraction in a metamaterial composed of an array of SRRs and metallic wires, thereby validating Veselago's theoretical predictions.

The unique properties of metamaterial have paved the way for numerous applications in diverse fields. Despite the significant progress in the research, several challenges must be addressed for practical implementation. Metamaterials with metallic components often exhibit high losses due to the absorption and scattering of electromagnetic waves by their meta-atoms. Reducing these losses and developing low-loss materials remains a critical research goal. Developing scalable and cost-effect fabrication techniques for metamaterials, particularly at optical frequencies, is essential for their widespread adoption. The integration of active components and the development of tuneable and reconfigurable metamaterials can expand their potential applications and enable dynamic control over electromagnetic properties.

The birth of metamaterials has had a profound impact on our understanding of electromagnetic wave propagation and manipulation. As research continues to address the challenges associated with metamaterials and explore new applications, these artificial materials have the potential to revolutionise various scientific and technological domains. The development of novel metamaterial design, fabrication techniques, and theoretical frameworks will undoubtedly shape the future of material science, electromagnetism, and optics, pushing the boundaries of what is possible in these fields.

1.3 Ripple Effects: Significance & Impact

As humanity stands at the precipice of a new era in optical technology, the exploration of these leading-edge materials holds the promise of revolutionising the way societies perceive and interact with the world around us. By transcending the limitations of conventional lenses and pushing the boundaries of human imagination, NIMs have the potential to unlock a treasure trove of advancements, benefits, and applications across a variety of fields.

The power of NIMs lies in their ability to address the most pressing challenges faced by conventional lenses in imaging systems: optical aberrations, inefficiencies, and the constraints imposed by traditional materials. By overcoming these hurdles, NIMs can give rise to a new generation of optical devices that could have profound implications for the development and advancement of emerging technologies, such as industry 4.0 vision, autonomous vehicles, remotes sensing, medical imaging, virtual and augmented reality, and even space exploration.

1.4 Ties to Innovation

This research is fundamentally connected to innovation engineering and innovation management, as it explores innovative materials and their potential applications while requiring effective strategies for successful implementation.

Innovation engineering is crucial in the design and simulation of NIM lenses, as it involved the integration of mathematics, optical physics, electromagnetic theory, material science, and engineering principles to overcome conventional lenses' limitations.

As this theoretical research progresses towards real-world applications, effective innovation management becomes vital to ensure the successful assessment of technology feasibility. Innovation management strategies should also address potential challenges and risks,

including technical obstacles, intellectual property concerns, regulatory compliance, and market dynamics.

1.5 Guiding the Reader: Objectives & Thesis Structure

This work proposes to investigate the central research question: "*Theoretically speaking, can negative refractive index lenses offer a tangible SWAP-C benefit to optical systems?"* To answer the question, the following objects are defined:

- *Chapter 4:* Mathematically explore the design parameters for negative index materials.
- *Chapter 5:* Compare singlet lenses of positive and negative indexed materials.
- *Chapter 6:* Explore a NIM optical system for an industry 4.0 application.

Broadly, the work in this thesis can be separated into two themes. Chapters four and five are aimed at establishing broad design methods for generalised NIM lenses. Chapter six is subsequently aimed at an application for three-dimensional imaging within an industry 4.0 setting. With Chapter 7 answering the research question.

2

BACKGROUND: UNRAVELLING THE LIGHT

2.1 OPTICAL INNOVATION

The journey of optical innovation is a narrative of human ingenuity and scientific breakthroughs. Historically, the field of optics primarily revolved around the study of visible light and its manipulation through lenses, mirrors, and prisms. The earliest known optical artefacts, such as the Nimrud lens, date back to Assyria around 750 BC, suggesting a rudimentary understanding of light manipulation. The subsequent eras witnessed seminal works, notably by scholars like Ibn al-Haytham in the 11th century, who profoundly influenced the understanding of light and vision with his 'Book of Optics'. The Renaissance period marked significant advancements with figures like Kepler and Newton making groundbreaking contributions to the field. Kepler's works on the laws of refraction and Newton's experiments with prisms laid the foundational principles of geometric optics.

The 20th and 21st centuries have seen unprecedented advancements in optical technologies, largely driven by the fusion of optical studies with quantum mechanics and electromagnetism. The invention of lasers in the 1960s marked a pivotal moment, opening new

realms in both theoretical and applied optics. The development of fibre optics revolutionized telecommunications, and the advent of digital imaging technologies transformed photography and microscopy. More recently, the exploration of photonics at the nanoscale has led to the emergence of metamaterials, which have extraordinary optical properties not found in natural materials. These include the ability to bend light in unusual ways, leading to the development of superlenses that can surpass the diffraction limit of conventional lenses.

The conceptual leap to NIMs is a direct consequence of these recent optical innovations. NIMs are engineered at a subwavelength scale to exhibit a negative refractive index, a property not observed in naturally occurring materials. The theoretical foundations for NIMs were laid by Veselago in 1968, but it was not until the early 21st century that practical demonstrations in the microwave spectrum were achieved. The potential of NIMs in optical systems is vast, promising breakthroughs in imaging, sensor technology, and even cloaking devices. The ongoing research into the optical application of NIMs is a testament to the dynamic and ever-evolving nature of optical innovation, constantly pushing the boundaries of what is theoretically and practically possible in the manipulation of light.

2.2 Electromagnetic Theory

Electromagnetic Spectrum

The electromagnetic (EM) spectrum encompasses a broad range of wavelengths and frequencies, of which visible light is a narrow, yet fundamental component. Understanding the EM spectrum is vital in the realm of optical systems, as it forms the basis for analysing light interactions with materials and the design of optical devices.

The spectrum begins with radio waves, known for their extensive use in communication systems due to their long wavelengths. Advancing through the spectrum, there are microwaves

and the infrared region. The infrared spectrum, though not visible to the human eye, is pivotal in applications like thermal imaging. Thermal cameras, for instance, utilise the infrared spectrum to detect heat emitted by objects, enabling the visualization of temperature variations, which is essential in various fields, including surveillance and wildlife research.

The visible spectrum, positioned between the infrared and ultraviolet regions, is the range that the human eye can perceive, approximately spanning from 380 to 750 nanometres. Beyond this, ultraviolet light has applications in sterilisation and photolithography, owing to its higher energy levels.

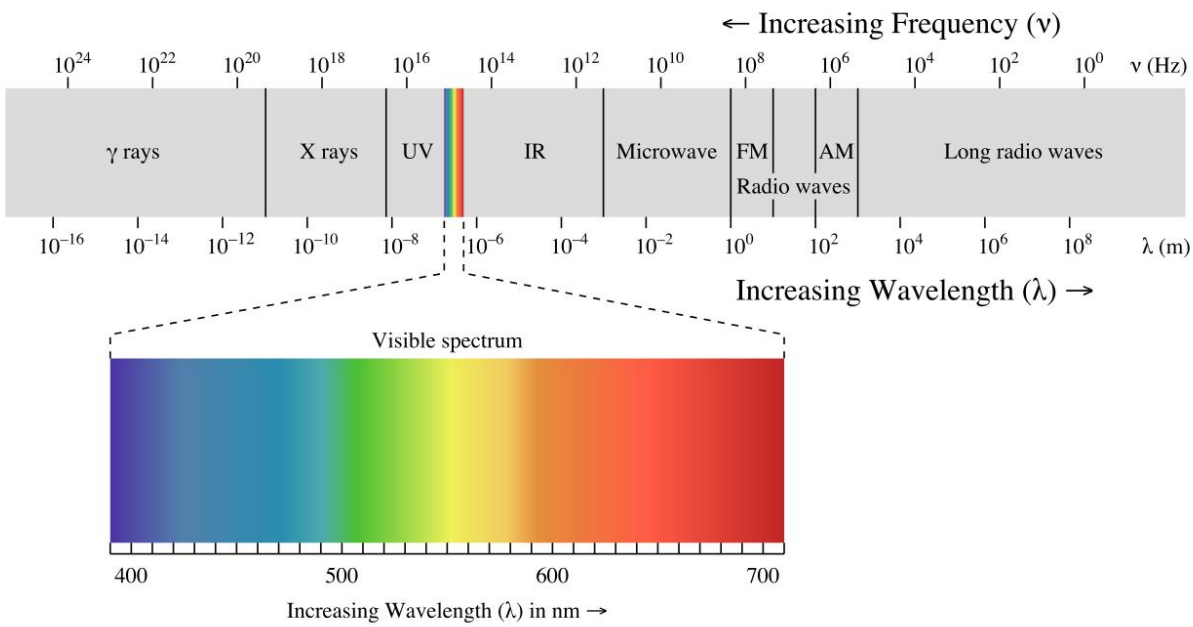

Figure 2.1. The discrete breakdown of the electromagnetic spectrum with the visible spectrum highlighted.

MAXWELL'S EQUATIONS

Maxwell's Equations, formulated by James Clerk Maxwell in the 19th century, are pivotal in the study of electromagnetic theory, particularly in understanding light propagation. The four equations describe how electric and magnetic fields are generated and altered by each other and

by charges and currents. They form the foundation upon which the modern understanding of light is built.

The electromagnetic field is represented by two vectors: the electric field vector (E) and the magnetic induction vector (B). These vectors are typically functions of time (t) and spatial coordinates (R). When the time variable is not present, these fields are referred to as static fields. If the spatial coordinates are not involved, the field is homogeneous. Maxwell's equations also incorporate the displacement field (D) and the magnetising field (H). These are connected to the electric and magnetic fields, as well as to bound charges and currents, though the constituent equations. The constituent equations include the permittivity (ε_0) and permeability (μ_0) of free space.

Table 2.1. Maxwell's equations.

	Differential Form	**Integral Form**
Faraday's law	$\vec{\nabla} \times E = -\frac{\partial B}{\partial t}$	$\oint_C E \cdot d\vec{l} = -\frac{d}{dt}\int_S B \cdot \hat{n}\, da$
Ampere-Maxwell law	$\vec{\nabla} \times H = \vec{J} + \frac{\partial D}{\partial t}$	$\oint_C H \cdot d\vec{l} = I_{enc} + \frac{d}{dt}\int_S D \cdot \hat{n}\, da$
Gauss's law for electric field	$\vec{\nabla} \cdot D = \rho$	$\oint_S D \cdot \hat{n}\, da = q_{enc}$
Gauss's law for magnetic fields	$\vec{\nabla} \cdot B = 0$	$\oint_S B \cdot \hat{n}\, da = 0$
	Electric Field	**Magnetic Field**
Material equations	$D = \varepsilon_0 E + \vec{P}$	$B = \mu_0 H + \vec{M}$
Wave Equations	$\nabla^2 E = \varepsilon_0 \mu_0 \frac{\partial^2 E}{\partial t^2}$	$\nabla^2 B = \varepsilon_0 \mu_0 \frac{\partial^2 B}{\partial t^2}$

These equations not only describe the behaviour of static electric and magnetic fields but also how they evolve and propagate as electromagnetic waves. In the context of light propagation, Maxwell's Equations explain how light waves, which are oscillating electric and magnetic fields, travel through different media and interact with materials. They provide the theoretical

underpinning for understanding the wave nature of light, an essential aspect in the study of optics and the development of optical systems.

WAVE PROPAGATION

The propagation of light waves through various media is a critical concept, governed by the principles of electromagnetic theory. Light, an electromagnetic wave, traverses through different media with varying behaviours, fundamentally altering the performance of imaging systems.

When light travels through a vacuum, it moves at its maximum velocity, approximately 299,792 km/s, a constant denoted by *c*. The speed and behaviour of light alter significantly when it transitions into media such as air, water, or glass. This change in speed, coupled with the direction of light, is governed by Snell's Law: $n_1 \sin\theta_1 = n_2 \sin\theta_2$, with n_1 and n_2 are the refractive indices of the two media, and θ_1 and θ_2 are the angles of incidence and refraction, respectively. This refraction phenomenon is fundamental in lens-based imaging systems, such as cameras and microscopes, where light is bent to focus images.

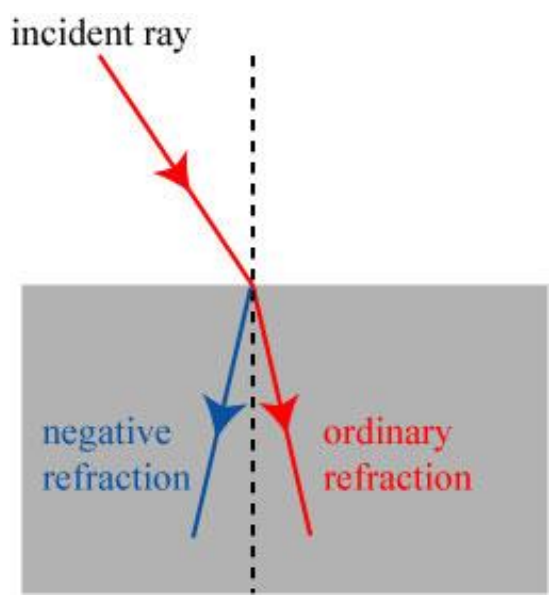

Figure 2.2. Snell's law of refraction illustrated for an ordinary case (positive index) and an unconventional case (negative index).

2.3 Optics

Evolution of Optics

The evolution of optics over the centuries is elegantly encapsulated in figure 2.3, which outlines the progression and convergence of different optical theories and technologies from the 1800s to the present day.

In the 1800s, the field of optics was predominantly governed by the principles of geometric optics, focusing on the propagation of light in terms of rays. This classical approach was foundational for the initial understanding of how light interacts with materials, leading to the development of lenses, mirrors, and the study of optical phenomena such as refraction and reflection.

As the field advanced into the wave theory of light, or wave optics, in the late 19th century, the focus shifted to understanding light as a wave phenomenon. This was spurred by the recognition of light's wave-like behaviours, such as interference and diffraction, which could not be explained by geometric optics alone.

The advent of the 20th century marked a significant shift with the introduction of quantum optics, which brought a deeper understanding of light at a microscopic level, considering its particle-like properties as photons.

Moving into the 2000s, figure 2.3 illustrates the merging of these disciplines into what is known as classical optics, which encompasses both geometric and wave optics. This comprehensive approach allows for a full description of light behaviour from macroscopic to microscopic levels, applicable in a variety of modern optical technologies.

Additionally, the figure indicates the emergence of structured quantum optics, a field that combines the principles of quantum optics with spatially structured electromagnetic fields. This

integration points to a sophisticated approach to manipulating photons and light fields, enabling advancements in quantum computing, secure communications, and high-precision metrology.

The overlapping of these fields in the figure underscores the interdisciplinary nature of modern optics, where understanding light requires a holistic approach that encompasses its particle-like and wave-like characteristics, its interaction with matter, and its quantum mechanical aspects. This convergence has facilitated groundbreaking technologies in imaging, communications, and computation, driving forward the frontier of optical research and applications.

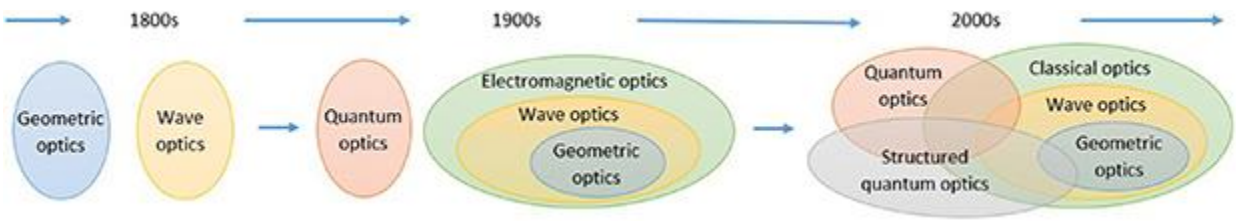

Figure 2.3. Discrete areas of optical physics through time.

Geometrical Optics

The general physics of light encompasses a broad spectrum of phenomena, marked by its dual character exhibiting both particle-like and wave-like properties. In the realm of geometric optics, this complexity is distilled into a more tractable form through the concept of a ray. This abstraction not only simplifies the analysis but also aids in the practical design and understanding of optical systems.

A ray in geometric optics is an idealised representation that streamlines the inherent properties of light into a singular, directed path. This simplification disregards the wave nature of light, focusing instead on its linear trajectory through different mediums. The utility of this approach lies in its ability to accurately model the behaviour of light in a wide array of optical systems, from simple lenses to complex imaging apparatus.

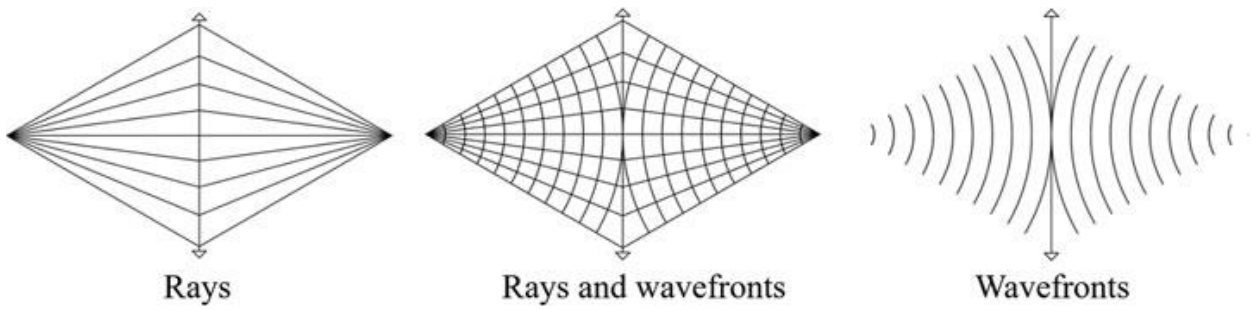

Figure 2.4. Demonstration of Ray optics formulated from the perpendicular of the wavefront.

Central to the understanding of ray trajectories in geometric optics is Fermat's Principle. This principle articulates that the optical path length of any ray, defined as the product of distance and the refractive index, attains a stationary point relative to adjacent paths within a local neighbourhood. Mathematically, Fermat's Principle can be expressed as:

$$\delta \int_{A}^{B} N(s) ds = 0$$

where δ represents the variation in the optical path length, *N(s)* is the spatially dependent refractive index, and *ds* denotes an infinitesimal element of the path between points A and B.

The refractive index, *N(s)*, is a dimensionless quantity pivotal in the study of geometric optics. It characterises how much the velocity and wavelength of light are altered when propagating through different materials. The refractive index is not merely a property of the material but can vary with factors such as wavelength, temperature, and spatial distribution within the medium. This variation has profound implications on the behaviour of rays, influencing phenomena such as refraction, dispersion, and total internal reflection.

The principles of geometric optics find extensive applications in the design and analysis of lenses, mirrors, and other optical elements. However, it is imperative to recognise the limitations of this approach. Geometric optics does not account for wave phenomena such as diffraction and interference, which become significant when the dimensions of the optical system approach the

wavelength of light. Hence, while geometric optics provides a robust framework for many practical applications, it is part of a larger tapestry of optical theories that together offer a comprehensive understanding of light.

Imaging Systems

Within the ambit of geometric optics, imaging systems serve as a critical application, translating abstract principles into tangible technology. Central to the operation of these systems is the concept of stigmatic imaging, wherein there is a direct correspondence between points in the object space and their image counterparts. This relationship is quantified by the magnification factor, m, encapsulated in the relationship $i' = mi$, where i' is the image point and i the object point.

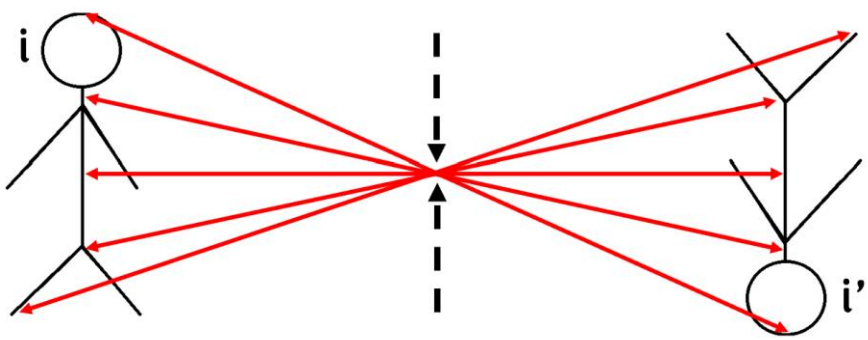

Figure 2.5. Example of stigmatic imaging via a tiny aperture with a unity magnification.

The camera obscura exemplifies the fundamental optical system, achieving theoretically perfect stigmatic imaging under the condition of an infinitesimal aperture. This perfection is, however, constrained by the practical limitations of resolution and light capture—key parameters that are crucial for the efficacy of modern imaging applications. By enlarging the aperture, we enable a greater collection of light, enhancing the system's resolution due to the diffraction limit, albeit this increase is moderated by the size of the aperture stop which delineates the maximum aperture of the system to prevent aberrations.

The focal length of a lens is a defining characteristic of imaging systems, indicating the distance at which a sharp image of a distant object can be produced. It fundamentally influences the field of view and magnification of the system. The focal power, the inverse of focal length, offers a concise metric of the system's ability to converge or diverge light.

ABERRATIONS

Chromatic Aberrations

Monochromatic Aberrations

Table 2.2. The five Seidel aberrations.

Aberration	Description	Representation
Spherical	Occurs when light rays from the periphery of a lens focus at a different point than those near the centre. The result is a blurred image, as not all rays converge at the same focal point. Spherical aberration is inherent in spherical lenses and mirrors because their shape causes light rays to bend differently depending on their distance from the optical axis.	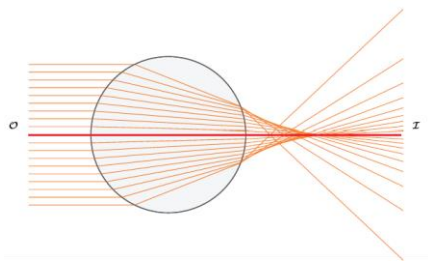
Coma	Appears as an asymmetrical, comet-like blur in the image, extending away from the optical axis. It occurs when light rays from an off axis point source are focused not into a single point but into a series of points, varying in radial distance from the optical axis. This aberration becomes more pronounced at wider apertures and with light that enters the lens from off-centre positions.	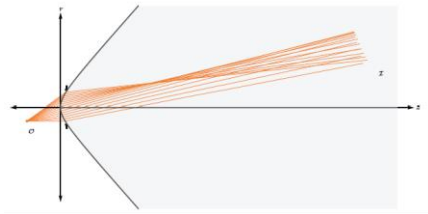

Astigmatism	Occurs when light from a point source does not focus to a single point on the image plane, due to the varying focal length of different meridional planes in the lens. Instead, it forms two-line foci at perpendicular orientations, leading to an image that is sharp in one direction but blurred in the perpendicular direction. Astigmatism is often observed in images taken with cylindrical or toric lenses.	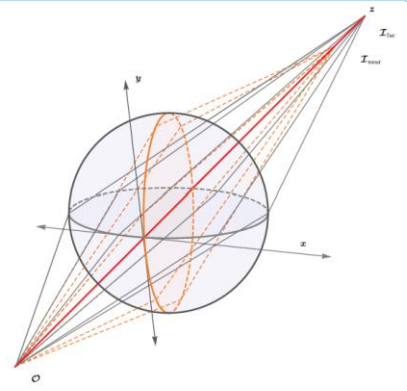
Petzval	Unlike the previous aberrations that relate to the quality of focus at a point, field curvature refers to the shape of the image plane. Instead of being flat, the focused image plane is curved, causing the edges of the image to appear out of focus when the centre is in focus, or vice versa. This means that a flat object cannot be sharply focused across the entire field of view simultaneously.	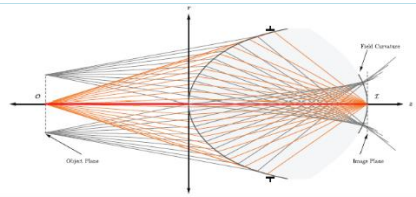
Distortion – *Pincushion*	Causes straight lines to appear curved or bent in the image, altering the geometric shape of objects. It comes in two main forms: barrel distortion, where lines bow outward from the centre, and pincushion distortion, where lines bend inward. Distortion does not affect the sharpness or focus of the image but changes the spatial relationship of objects within the field of view.	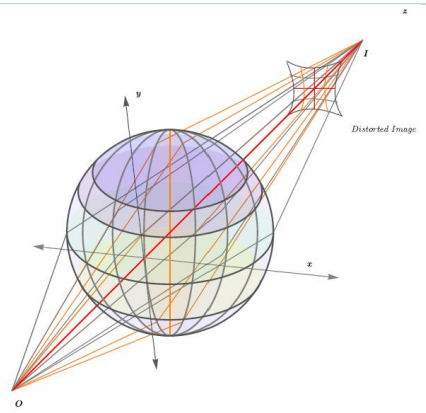
Distortion - *Barrel*		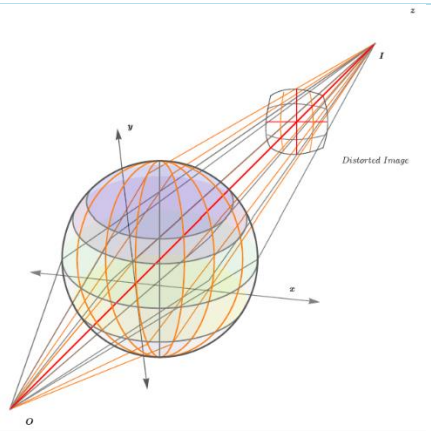

3

METHODOLOGY: CRAFTING THE VISION

3.1 ART, ENGINEERING & SCIENCE

Optical design is an interdisciplinary field that blends the scientific principles of optics with the creativity and aesthetics of art. This topic involves devising a system of optical components to fulfil a specified set of optical requirements. This process typically incorporates geometrical optics and optimisation, followed by an in-depth analysis of optical performance to determine the suitability of a given optical solution. The suitability of an optical construction is assessed by examining numerous input parameters and minimising a *merit function* based on key performance parameters.

The complex and non-linear nature of the optical design *merit function* renders the problem difficult to solve. Optical design software like Zemax® and CodeV® employs optimisation techniques, such as the Levenberg-Marquardt (damped least squares) algorithm, to find solutions to optical imaging problems. However, these algorithms have limitations, including difficulties in determining the convergence of global optimisation routines and the need for manual intervention in higher-level design decisions.

Optical design is frequently referred to as both an art and a science. Successful execution of a design task requires not only a deep understanding of the underlying optical theory but also significant intuition into the form and structure of optical systems.

The artistic aspect of optical design comes into play when considering the aesthetic and ergonomic factors of an optical system. Balancing form and function are crucial for creating systems that are not only effective but also visually appealing and user-friendly.

In addition to the artistic and scientific aspects, real-world optical design tasks necessitate engineering knowledge. Desired performance from an optical specification may not be feasibly achievable with existing materials, processes, and timescales. Pragmatic compromises with stakeholders and interdisciplinary collaboration within the design team are often required to produce an optical system with optimal performance at a viable cost.

3.2 Optical Design Process

The methodology for designing a lens for an optical imaging system involves a structured and sequential process that ensures the creation of high-performance lenses that fulfil specific requirements. This process consists of several stages, with each step building on the previous one to guarantee that the ultimate design is both optimized and capable of being manufactured. However, because the NIMs discussed in this dissertation are theoretical materials yet to be realised, the design-for-manufacturing component will be absent. The following provides an overview of the lens design methodology:

1. *Defining Specifications*: The initial stage of the lens design process entrails identifying the lens type required for the optical imaging system. This involves stipulating the desired focal length, aperture size, field of view, image quality, and other pertinent criteria. These specifications play a vital role in directing the remainder of the design process.
2. *Initial layout and thin lens predesign*: the subsequent step encompasses generating a preliminary layout of the optical system and devising a simplified lens model that adheres to the specified criteria. This initial design offers valuable insight into the properties of the lens under development and enables the designer to foresee potential issues that may emerge in later stages of the process.
3. *Creation of detailed surface model*: During this phase, a comprehensive surface model is generated based on the simplified lens model. The aberration coefficients are determined, and the simplified lenses are assigned thickness while ensuring that the paraxial properties of the initial design and colour correction are conserved. The surface contributions to Seidel aberrations can be employed to decide which parameters will serve as variables in the optimisation stage,
4. *Refinement through optimisation*: The optimisation phase concentrates on enhancing the lens design to attain the desired performance level outlined earlier. This may involve modifying lens shapes, materials, or distances between elements. Optimisation can be executed using various methods such as manual trail-and-error or sophisticated optimisation algorithms.
5. *Production preparation and tolerancing*: Following optimisation, the lens design must be readied for manufacturing. This stage involves evaluating the design's sensitivity to fabrication errors and estimating the resulting impact on lens performance. An efficient tolerancing method ensures that the design can be produced with acceptable variations in the lens component while maintaining the desired optical performance.

It is crucial to note that this lens design methodology concentrates on the prescription of optical components and does not consider opto-mechanical aspects or optical fabrication technologies, including metrology. These aspects are essential for the successful integration of a lens design into a final, functional optical imaging system.

3.3 Selection of Negative Index Glass Materials

The selection of appropriate NIMs is a crucial step in the investigation of their performance in imaging systems. As this study aims to explore the potential benefits and drawbacks of NIMs, it is imperative to base the selection of these materials on sound theoretical principles. In *Chapter 4*, the author delves into the electromagnetic principles and optical physics theory required to theoretically determine the characteristics of suitable NIMs.

Electromagnetic principles, such as Maxwell's equations, govern the behaviour of light in different media, and they play a critical role in understanding the interaction between light and NIMs. By analysing the electric and magnetic fields, as well as their relationships with the permittivity and permeability of materials, an insight can be gained into the unique properties of NIMs.

Optical physics theory also plays a significant role in determining the characteristics of NIMs. Snell's law, which governs the refraction of light at the interface of two media, will be adapted to account for the NIMs. Additionally, the dispersion relation, which describes the relationship between the refractive index and the frequency of light, will be explored to understand how these materials may be tailored for specific applications in imaging systems.

By combining the principles of electromagnetic theory and optical physics, the author will derive the properties of generalised NIMs. This theoretical foundation will guide the selection of materials for the design and simulation of imaging systems, ensuring that the research is grounded in established scientific principles and that the result obtained are both valid and meaningful.

3.4 DESIGN & SIMULATIONS

The design and simulation of imaging systems incorporating NIM lenses are essential steps in assessing their performance and potential applications. To perform these tasks, two software tools will be employed, MATLAB® and Zemax®.

MATLAB®, a high-level programming language and interactive environment for numerical computing, will be used to develop custom algorithms for the calculation of the artificial material's optical refractive indices.

Zemax® offers a comprehensive suite of tools for designing, analysing, and optimising optical systems. Zemax® will enable the creation of realistic models of imaging systems, considering factors such as lens geometry, material properties, and system configurations. The software's powerful simulation capabilities will permit the assessment of the performance of these systems, including the effects of aberrations and other factors that may influence image quality.

By leveraging the capabilities of MATLAB® and Zemax®, the author will design and simulate optical systems that incorporate NIM lenses, providing valuable insights into their performance and potential advantages over conventional lenses.

3.5 LIMITATIONS

The use of NIMs for lenses within optical systems, while conceptually promising, is accompanied by several significant challenges. One major drawback is the inherent material loss due to absorption, particularly at optical frequencies, which may limit their effectiveness in practical applications. The absorption properties reduce the quality and quantity of transmitted light. In this study, however, to simplify the exploration and focus more closely on the impact of negative refraction alone, the effects of absorption are being ignored.

Furthermore, typical NIMs exhibit anisotropic (direction-dependent properties), and inhomogeneous (properties that change with location within the material) behaviours. These characteristics further complicate their design and implementation, especially in an optical system. However, for the purpose of this study, it will be assumed that the NIMs are linear, isotropic, and homogeneous. Additionally, the physical design of the NIM metamaterial unit-cell's will not be evaluated.

In reality, these assumptions may not hold true and could oversimplify their actual behaviour. Assuming isotropy and homogeneity overlooks the directional dependence and spatial variation of their properties. Nonetheless, these assumptions allow this research to focus on the base properties of NIMs and their theoretical applications.

.

4

MATHEMATICAL CHARACTERISATION: INVERTING THE SPECTRUM

4.1 BIRTH OF NEGATIVE INDEX GLASSES[1]

When examining how light interacts with a material, it is first assumed that Maxwell's equations can supply the answer. This set of equations can lead to intriguing outcomes. To simplify this concept, imagine a neutral particle composed of a positively charged nucleus and a surrounding negatively charged electron cloud. This electron cloud model deviates from the Bohr model, which focuses on electron orbits in the context of quantum mechanics.

The electron cloud model emphasizes that it is impossible to pinpoint an electron's exact location at any given moment. Instead, it offers a probability that the electron is more likely to be found in certain areas. When an electric field is applied to the particle, the electron cloud shifts relative to the nucleus. As a result, a negative charge appears on one side of the particle, while a

[1] The work and mathematical derivations discussed in subsection 4.1 have been directly taken from the authors' *Doctor of Philosophy* thesis, titled "Shift-free wide-angle metamaterial narrowband filters for anti-laser striking applications" (Monks, 2020).

positive charge emerges on the opposite side. This creates an electric dipole, a phenomenon referred to as polarisation.

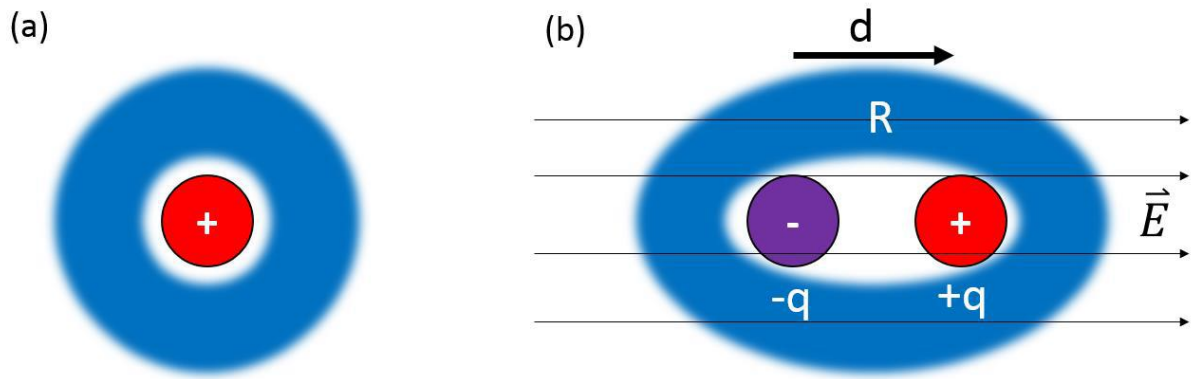

Figure 4.1. (a) Neutral particle without an external electric field. (b) Particle displaying dipole properties due to the external electric field.

The electric dipole of a system is described by the following equation.

$$\vec{d} = \sum_i \vec{r}_i q_i \rightarrow \vec{d} = \vec{R}q$$

Where $\vec{R}$ is the sum of ith $\vec{r}$ and denotes the distance between the two charges, and q is the charge of the system.

The polarisation and magnetisation refer to the density of electric and magnetic dipole moments induced by external fields. Consequently, polarisation is dependent on the electric field, while magnetisation is influenced by the magnetic field. These concepts are essential in understanding how materials respond to and interact with external electric and magnetic fields, which can have significant implications for various applications and technologies.

$$\vec{P}(\vec{E}) = \chi_e \vec{E}$$

$$\vec{M}(\vec{H}) = \chi_m \vec{H}$$

Where $\vec{P}$ and $\vec{M}$ denote the polarisation and magnetisation, and χ_e and χ_m express the electric and magnetic susceptibility which describe the degree to which a material can be polarised

or magnetised. Note that the constants have been removed because they are usual zero except for specialist materials like pyroelectric materials. Additionally, the non-linear terms have been removed.

The permittivity and permeability properties can be represented using a complex formula, which may yield a complex solution. In general optics, the magnetisation is typically negligible, therefore, only the permittivity requires consideration. The complex function of permittivity (ε) enables it real part to represent the material's polarisation, while the imaginary part accounts for any loss within the material. This distinction is crucial for understanding how various materials respond to and affect electromagnetic fields in different applications.

$$\varepsilon = 1 + \chi_e$$

Material behaviours are determined by how the electrons interact with the valence and conduction band, and the interband and intraband transitions of electrons. To understand how electrons influence refractive index, a time-varying electric field can be mathematically applied.

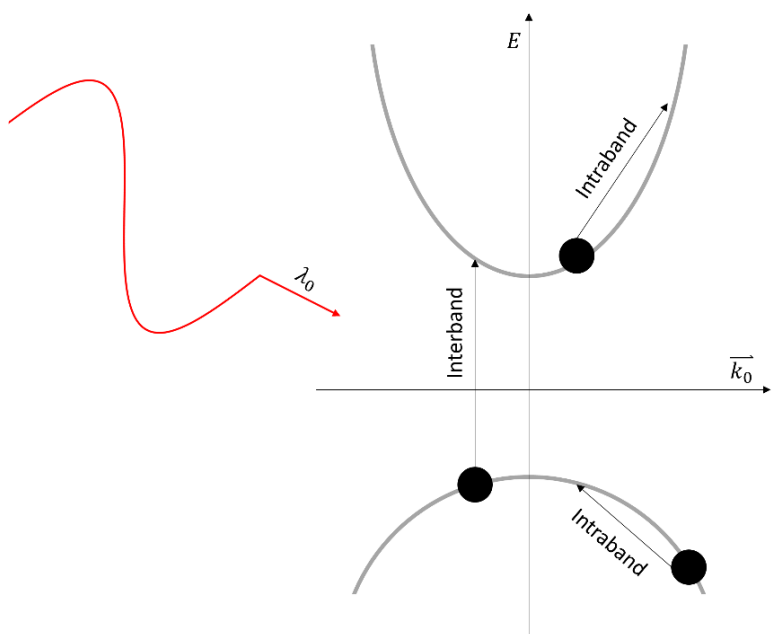

Figure 4.2. A simplistic representation of interband electron transitions vs intraband electron transitions.

The net force on an electron that is bound to its ion core for a given material can be defined by the equation of motion by comparing bound charges to a mass on a spring.

$$m\frac{\partial^2\vec{r}}{\partial t^2} = q\vec{E} - G\frac{\partial\vec{r}}{\partial t} - C\vec{r}$$

Where m is the mass and q is the charge of an electron, $\vec{r}$ described the electrons displacement from an equilibrium state, $\vec{E}$ is the electric field, G is the dampening constant and C is the restoring force. The three terms on the right-hand side of the equation, each have their own individual role to play in describing the net force. The first term denotes the force experienced by the electron with an applied field, the second term signifies the dampening force resulting from electron scattering and the third term represents the electrons attraction to the ion core. By allowing the electron to assume a harmonic oscillation at the same frequency as the electric field, $\vec{r} = \overrightarrow{r_0}e^{i\omega t}$ and $\vec{E} = \overrightarrow{E_0}e^{i\omega t}$ can be substituted.

$$-\omega^2 m\vec{r} = q\vec{E} + i\omega G\vec{r} - C\vec{r}$$

By adapting the previous equation to make the driving term the subject, the equation of motion becomes more evident.

$$q\vec{E} = C\vec{r} - i\omega G\vec{r} - \omega^2 m\vec{r}$$

Allowing the subject to be the driving term, the three terms become distinguishable, as does the description of their roles in the system. The three terms available now define low frequencies, high frequencies, and resonant conditions.

At low frequencies, the restoring force is maintained by the force applied from the electric field, therefore, ω becomes negligible.

$$q\vec{E} = C\vec{r}$$

At high frequencies, the electron effectively becomes a free particle where there is no force acting to restore equilibrium or dampen the motion. This is a result of the dominating ω^2 term.

$$q\vec{E} = -\omega^2 m\vec{r}$$

During the resonant period, the dampening term directs the result and actions a limitation to the velocity, causing the displacement of the electrons that lags the electric field.

$$q\vec{E} = -i\omega G\vec{r}$$

Following the analytical breakdown of the terms, rearranging the equation of motion to make the charge displacement the subject enables a preview of materials permittivity.

$$\vec{r} = \frac{q\vec{E}}{-i\omega G + C - \omega^2 m} = \frac{\left(\frac{q\vec{E}}{m}\right)}{-i\omega\frac{G}{m} + \frac{C}{m} - \omega^2}$$

Grouping certain components together, namely $\gamma = G/m$ and $\omega_0 = \sqrt{C/m}$, where ω_0 is the resonant frequency, the subsequent equation can be obtained.

$$\vec{r} = \frac{\left(\frac{q\vec{E}}{m}\right)}{-i\omega\,\gamma + \omega_0 - \omega^2}$$

The significance of the previous equation shows that the position of the electron as a function of time, is directed by the dampening term when under resonance.

To obtain the frequency dispersive permittivity, ε_r, for a given material, the polarisation can be expressed as a density of discrete dipole moments, with the electric susceptibility represented as a relation to the materials permittivity, $\chi_e = \varepsilon_r - 1$.

$$\vec{P} = N\vec{p} = Nq\vec{r} = \varepsilon_0\chi_e\vec{E} = \varepsilon_0(\varepsilon_r - 1)\vec{E}$$

Where $\vec{P}$ is the dipole density and $\vec{p}$ is the dipole moment that is a product of displacing and electron with charge q at a distance of $\vec{r}$ from the position of equilibrium, and N is the number of atoms per unit volume.

The expression for the relative permittivity of a material can be derived by substituting the two previous equations.

$$\varepsilon_r = 1 + \frac{\left(\frac{Nq^2}{m}\right)}{\varepsilon_0(-i\omega\,\gamma + {\omega_0}^2 - \omega^2)}$$

The common form for expressing the permittivity is often denoted with the plasma frequency, $\omega_p = \sqrt{\frac{Nq^2}{\omega_0 m}}$.

$$\varepsilon_r = 1 - \frac{\omega_p^2}{\omega^2 - \omega_0^2 + i\omega\gamma}$$

Similarly, the permeability can be derived, leading to the following notation.

$$\mu_r = 1 - \frac{\omega_p^2}{\omega^2 - \omega_{0m}^2 + i\omega_m\gamma_m}$$

Where the subscript m denotes the magnetic response.

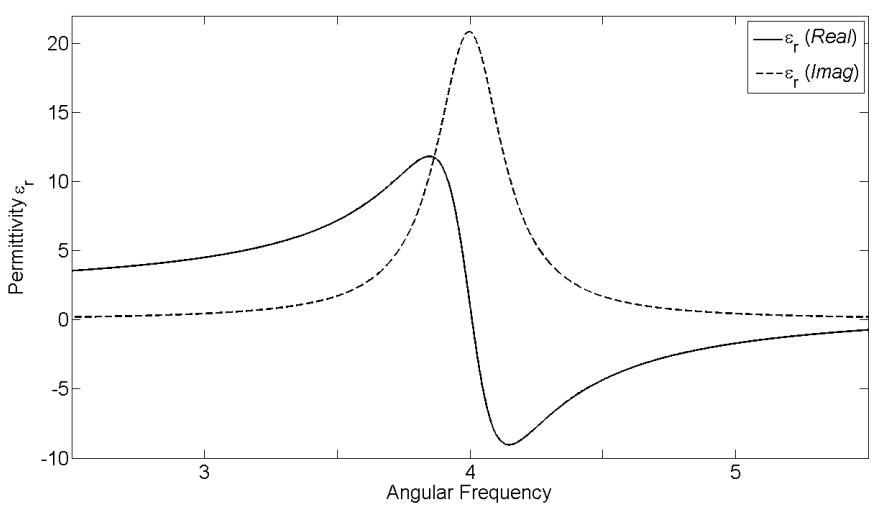

Figure 4.3. The Drude-Lorentz permittivity for a conjectural material with ω_0=4, ω_p=5, *and* γ=0.3.

The permittivity and permeability equations presented previously, are commonly known as the Drude-Lorentz model, and provide an excellent prediction for the behaviour of dielectric materials.

Similar to the Drude-Lorentz permittivity model, metals also ascribe to frequency-dependent behaviours. The behaviour of electromagnetic interactions in metals is determined by the movement of free electrons within their crystalline structure. This leads to a unique application of Drude-Lorentz model, known as the Drude model, where the restoring force or spring constant is eliminated due to the Coulomb's interaction between electrons and ion cores (i.e. $\omega_0 = 0$). The Drude model is particularly useful for characterising metallic media, as it focuses solely on free electrons. Omitting the restoring force is justified, given that the applied electric field has a strong interaction with the conducting electrons in metals.

$$\varepsilon_r = 1 - \frac{\omega_p^2}{\omega^2 + i\omega\gamma}$$

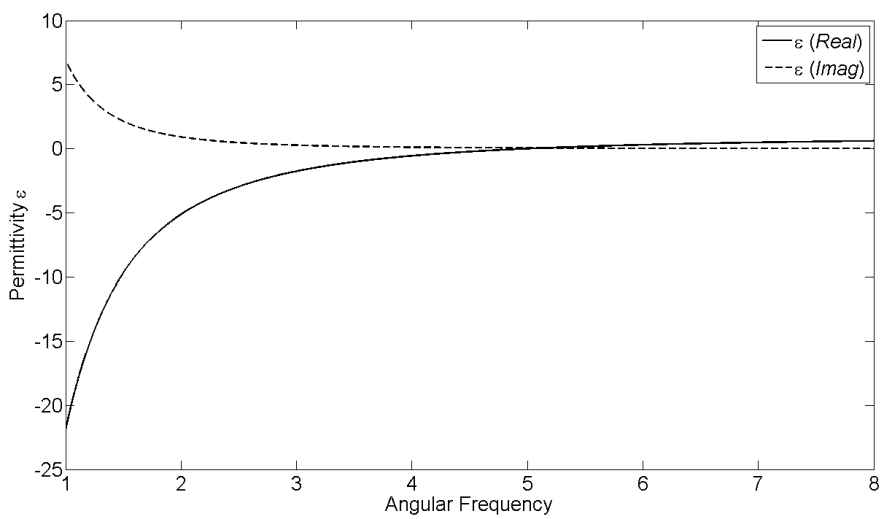

Figure 4.4. The Drude permittivity for a conjectural material with ωp=5, *and* Γ=0.3. The Plasmas Frequency is the point at which the real part switches from negative to positive.

A crucial aspect of the Drude model is the real part of the permittivity turning negative below the plasma frequency (ω_p). When the frequency is below ω_p, the material exhibits metallic properties because the electrons at its surface respond to the incoming field. This response results in out-of-phase oscillations of electrons that generate a reflected field. For instance, this phenomenon explains the yellowish hue observed in gold.

To develop a description of the refractive index in terms of the permittivity and permeability, a review of Maxwell's equations is once again required.

$$\nabla \times \vec{E} = -\frac{\partial \vec{B}}{\partial t}$$

$$\nabla \times \vec{B} = \varepsilon\mu \frac{\partial \vec{E}}{\partial t}$$

By taking the curl and combining of both sides of the above two equations, the following equation can be deduced.

$$\nabla \times \left(\nabla \times \vec{E}\right) = -\frac{\partial\left(\nabla \times \vec{B}\right)}{\partial t} = -\varepsilon\mu \frac{\partial^2 \vec{E}}{\partial t^2}$$

In general, for any vector $\vec{a}$:

$$\nabla \times (\nabla \times \vec{a}) = -\nabla^2 \vec{a} + \nabla \cdot (\nabla \cdot \vec{a})$$

In a vacuum, $\nabla \cdot \vec{E} = 0$. In this case the above equation becomes:

$$\nabla^2 \vec{E} = \varepsilon_0 \mu_0 \frac{\partial^2 \vec{E}}{\partial t^2}$$

Where ε_0 and μ_0 denote the permittivity and permeability of free space, respectively.

The above equation now represents the wave equation in three dimensions. Assuming that the material is linear, isotropic, and homogenous, the equation can be converted to a one-dimensional equivalence, the equation becomes:

$$\frac{\partial^2 \vec{E}}{\partial x^2} = \varepsilon_0 \mu_0 \frac{\partial^2 \vec{E}}{\partial t^2}$$

Differentiating with respect to x and t:

$$\frac{\partial^2 \vec{E}}{\partial x^2} = -\overrightarrow{E_0} \left(\frac{2\pi}{\lambda}\right)^2 \sin\left(2\pi \frac{x - ct}{\lambda}\right)$$

$$\frac{\partial^2 \vec{E}}{\partial t^2} = -\overrightarrow{E_0} \left(\frac{2\pi c}{\lambda}\right)^2 \sin\left(2\pi \frac{x - ct}{\lambda}\right)$$

And substituting back into the one-dimensional wave equation:

$$-\overrightarrow{E_0} \left(\frac{2\pi}{\lambda}\right)^2 \sin\left(2\pi \frac{x - ct}{\lambda}\right) = -\varepsilon_0 \mu_0 \overrightarrow{E_0} \left(\frac{2\pi c}{\lambda}\right)^2 \sin\left(2\pi \frac{x - ct}{\lambda}\right)$$

The above equation can be simplified and rearranged to express the speed of light in a vacuum, c.

$$c = (\varepsilon_0 \mu_0)^{-1/2}$$

As such, the free space permittivity and free space permeability can be replaced with a material's relative permittivity and relative permeability.

$$c_r = (\varepsilon_r \mu_r)^{-1/2}$$

Therefore, using the expression for c and c_r, the refractive index of a material can be expressed in terms of the permittivity and permeability, as it is the ratio of the velocity of light in a vacuum to its velocity in a specified medium.

$$n = \left(\frac{\varepsilon_0 \mu_0}{\varepsilon_r \mu_r}\right)^{-1/2}$$

Therefore:

$$n^2 = \varepsilon \mu$$

As discussed in *Chapter 1*, Veselago's famous paper suggested that negative refractive index of a material is given by:

$$n = -\sqrt{\varepsilon \mu}$$

4.2 DISPERSION DYNAMICS

Dispersion is the phenomenon where the phase velocity of a wave depends on its frequency. In optics, the term chromatic dispersion or chromatic aberration, refers to the phenomenon in which light of different wavelengths (colour) is refracted, or bent, by different amounts as it passes through a lens. This happens because the refractive index of the lens material changes with the wavelength of the light, leading to different propagation speeds for different wavelengths.

When light of different wavelengths passes through a lens, the lens material's variation in refractive index causes each wavelength to be refracted differently. As a result, the different colour components of a light beam do not all converge to the same point, which can lead to blurred or colour-fringed images. This is a major issue in many fields, such as photography, microscopy, and astronomy.

For standard optical materials, the refractive index will decrease with increasing wavelength (λ).

$$1 < n(\lambda_{red}) < n(\lambda_{green}) < n(\lambda_{blue})$$

Or generally:

$$\frac{dn}{d\lambda} < 0$$

There are two types of chromatic aberration, *as discussed in Chapter II, Section 2.3 Aberrations*:

1. Longitudinal Chromatic Aberration: This occurs when different wavelengths of light are focused at different distances from the lens (i.e., along the optical axis).
2. Lateral Chromatic Aberration: This happens when different wavelengths are focused at different positions at right angles to the optical axis, causing colour fringing at high-contrast edges within the field of view.

Quantitatively, chromatic dispersion in a lens is usually characterised by the Abbe number (V), which is a measure of the material's dispersion:

$$V = \frac{n_D - 1}{n_F - n_C}$$

Where n_D, n_F, and n_C are the refractive indices of the material for the Fraunhofer D (589.3 nm), F (486.1 nm), and C (656.3 nm) spectral lines respectively. A large Abbe number indicates lower chromatic dispersion.

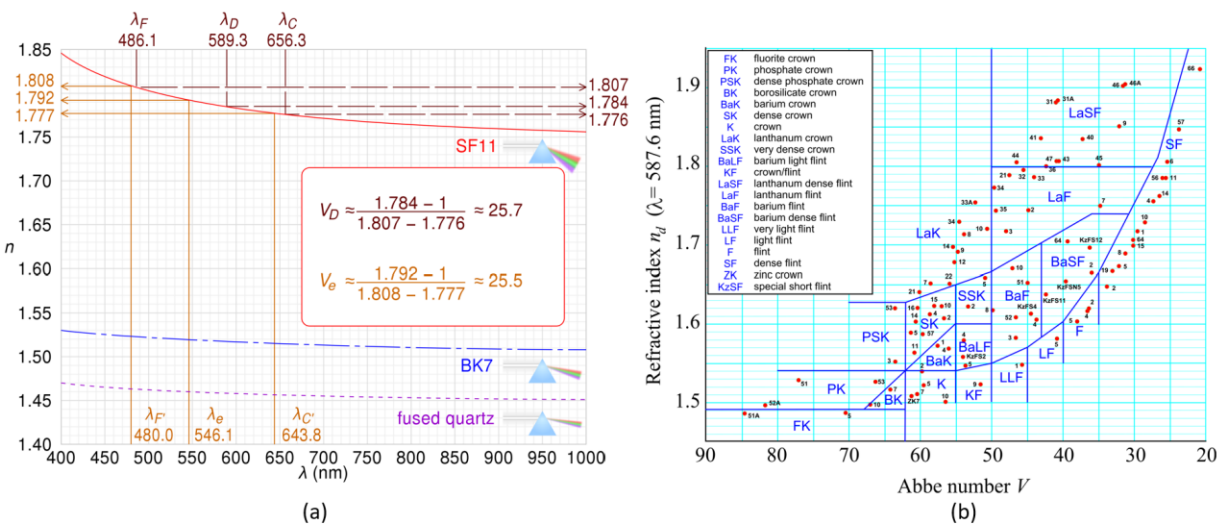

Figure 4.5. (a) The dispersion variation between three types of glass. (b) Abbe diagram with glass classifications.

One of the traditional ways to correct for this problem is using an achromatic doublet, which is a compound lens made up of two simple lenses with different types of glass.

This is where crown glass and flint glass come into the picture.

1. Crown Glass: This is a type of low-dispersion glass. It has a relatively low refractive index and low dispersion, which means that it bends light less and causes less separation of light into different colours than other types of glass.
2. Flint Glass: This is a type of high-dispersion glass. It has a higher refractive index and higher dispersion than crown glass, which means it bends light more and causes more separation of light into different colours.

In an achromatic doublet, a convex lens made of crown glass is usually paired with a concave lens made of flint glass. The crown lens refracts the light less but also disperses it less, while the flint lens refracts the light more but also disperses it more.

The key to the achromatic doublet's performance is that the two lenses are designed so that the chromatic dispersion of the flint glass lens cancels out the chromatic dispersion of the crown glass lens. In other words, the different colours of light that were spread out by the crown lens are brought back together by the flint lens.

The result is that two different wavelengths of light - typically red and blue - are brought to the same focus, significantly reducing the chromatic aberration of the lens system. This doesn't eliminate chromatic aberration (as there are more than two wavelengths in visible light), but it's a significant improvement over a singlet lens.

More complex systems, such as apochromatic lenses, use more elements and often different types of glass to bring even more wavelengths into the same focus, further reducing chromatic aberration.

The use of crown and flint glass in achromatic doublets was a major advancement in optical technology and is still used in many optical systems today, including camera lenses, microscopes, and telescopes. It is a practical and effective method of reducing chromatic aberration, improving the quality of the images produced by these systems.

Unlike conventional glass, NIMs are not found in nature and therefore must be engineered. One of the significant challenges with NIMs relates to their dispersion properties. In designing NIMs, the dispersive characteristics are not predetermined like conventional glasses, but must be defined and optimised during the design process. This is achieved by carefully manipulating the material’s permittivity and permeability profiles. In conventional optical materials, the magnetic

response is negligible, as such, it does not play a role in determining the refractive index. However, due to the unique nature of NIMs, it is possible to engineer artificial magnetic resonances in the material.

The Drude model, which describes the response of free electrons to an applied electromagnetic field, can be used to tailor the permittivity of NIMs. By adjusting the Drude permittivity profile with a specific plasma wavelength, the dispersive properties of the material can be controlled. Similarly, the Drude-Lorentz model, which accounts for both free and bound electron responses, can be used to tailor the permeability of NIMs. Through these models, the dispersion properties of these artificial materials can be managed, allowing for NIMs to be customised for a given optical system.

Reviewing the Drude and Drude-Lorentz models previously derived:

$$\varepsilon_r = 1 - \frac{\omega_p^2}{\omega^2 + i\omega\gamma}$$

$$\mu_r = 1 - \frac{\omega_p^2}{\omega^2 - \omega_{0m}^2 + i\omega_m\gamma_m}$$

Modifying the equations to separate out the plasma wavelength (λ_p), and enabling multiple magnetic resonances (λ_{mi}), the equations become:

$$\varepsilon_{eff}(\lambda) = \varepsilon_\infty - \frac{2\pi\left(c_0^2/\lambda_p^2\right)}{2\pi(c_0^2/\lambda^2) + i2\pi c_0(\gamma_e/\lambda)}$$

$$\mu_{eff}(\lambda) = \mu_\infty - \sum_{i=1}^{2} \frac{F_i 2\pi\left(c_0^2/\lambda_p^2\right)}{2\pi(c_0^2/\lambda^2) - 2\pi\left(c_0^2/{\lambda_{mi}}^2\right) + i2\pi c_0(\gamma_{mi}/\lambda_{mi})}$$

Where $\varepsilon_{eff}(\lambda)$ and $\mu_{eff}(\lambda)$ are the wavelength dependant effective permittivity and permeability, c_0 is the speed of light in free space, F_i is the filling factors, and γ_e and γ_{mi} are the electric and magnetic damping factors, respectively.

The imaginary parts of the permittivity and permeability are not considered for simplicity. However, it should be noted that the absorption loss must also be suppressed to ensure high transmission. The imaginary component of the effective permeability does not need to be removed because it will remain zero expect near and at the resonant wavelengths. Separating and removing the imaginary component of the effective permittivity:

$$\varepsilon_{eff}(\lambda) = \varepsilon_{\infty} - \frac{\omega_p^2}{\omega^2 + \gamma^2} + \cancel{i\frac{\omega_p^2 \gamma}{\omega^3 + \omega\gamma^2}}$$

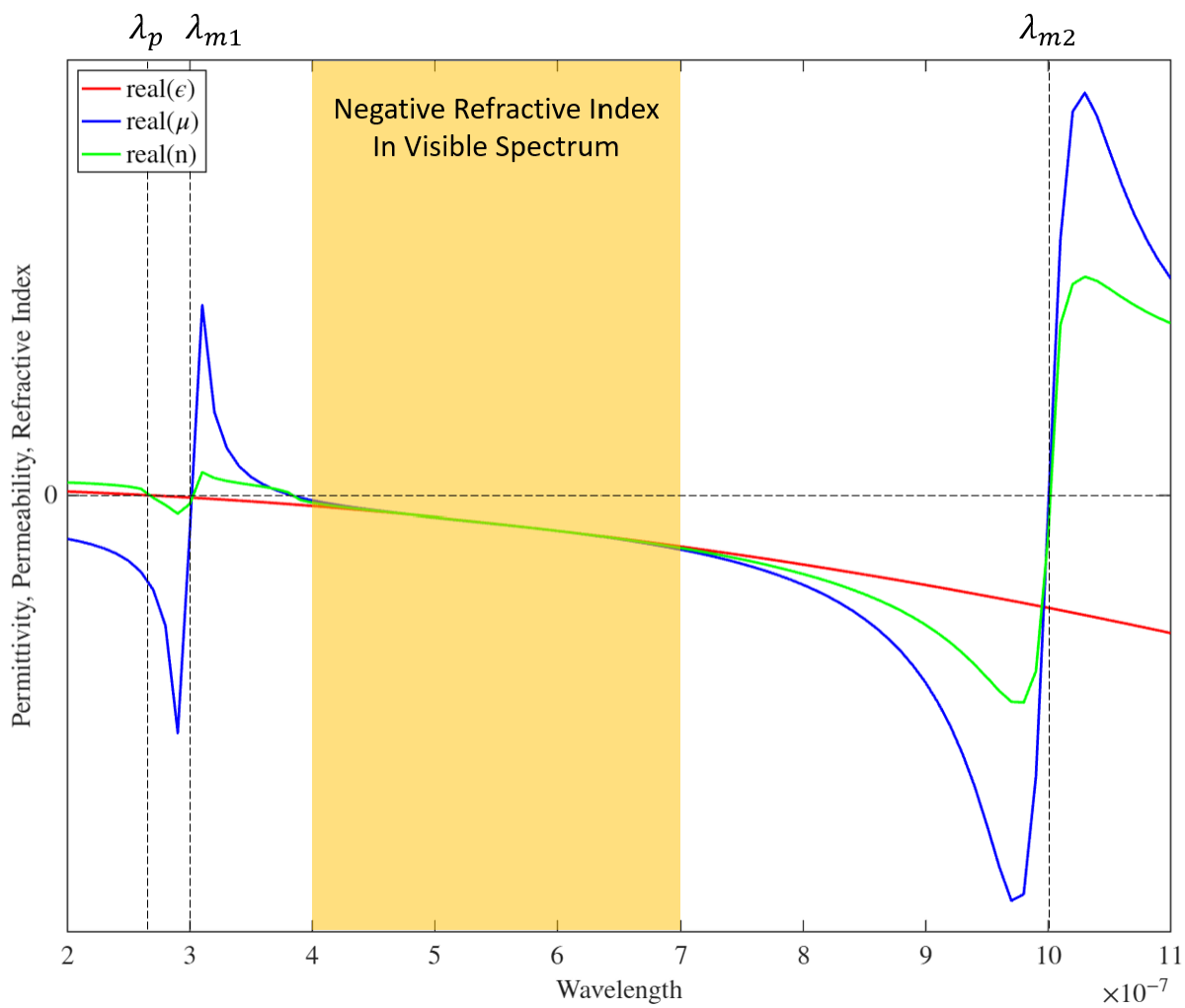

Figure 4.6. Example of real parts of the negative refractive index dispersion in visible spectrum, derived from the Drude and Drude-Lorentz model.

Realising the optical function of the NIM is achieved by carefully tuning the damping factors, plasma wavelength and magnetic resonance wavelengths to simultaneously satisfy a broadband negative refractive index.

Table 4.1. Material parameters for calculating the two artificial NIMs presented in *Figure 4.7*.

Material	ε_∞	ω_p	γ_e	μ_∞	λ_{m1}	λ_{m2}	γ_{m1}	γ_{m2}	F_1	F_2
NIM-A	-1.215	6.2832e15	1.1765e16	-1.557	200 nm	9 µm	1	1	0.15	0.0005
NIM-B	-1.217	6.2832e15	1.0000e16	-1.732	200 nm	9 µm	1	1	0.30	0.00035

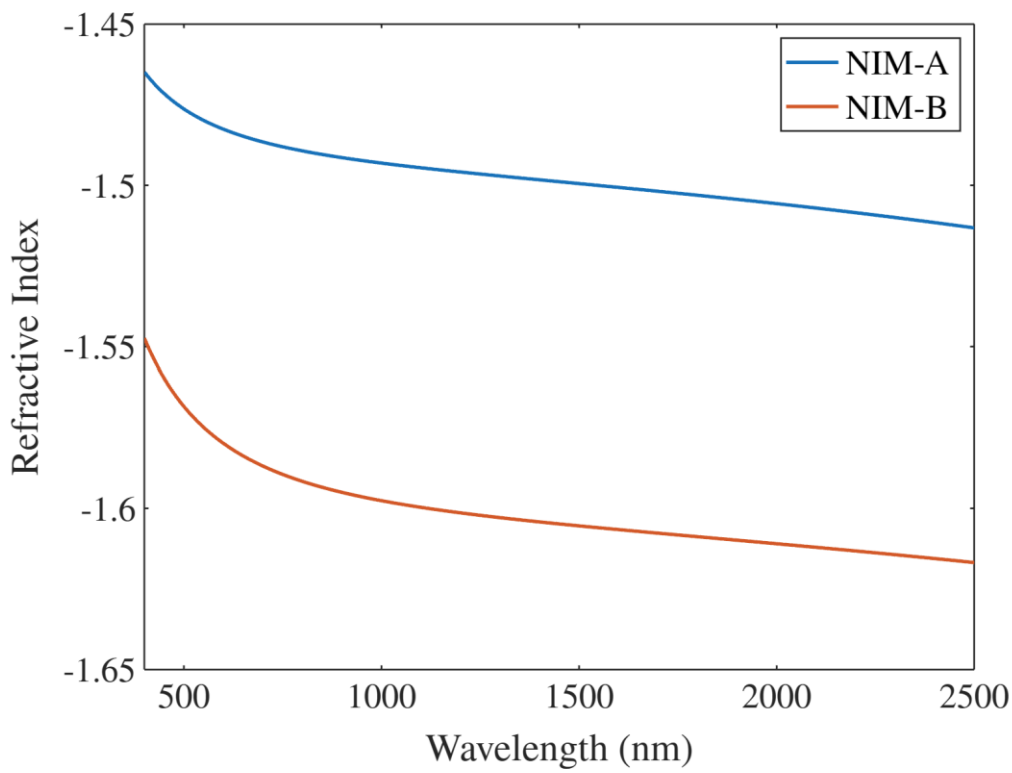

Figure 4.7. Example of two calculated negative refractive index materials with different dispersion behaviours, derived from the Drude and Drude-Lorentz model.

Table 4.2 presents the optical properties of the two artificial NIMs visually found in Figure 4.7, with the material parameters of Table 4.1.

Table 4.2. Properties of the two artificial NIMs.

Material	*Refractive Index at 589 nm*	*Abbe Number*
NIM-A	-1.48207	184.8153
NIM-B	-1.57887	143.9905

4.3 Chapter Summary

This chapter delved into the principle optical properties of NIMs. It began by exploring the interaction of light with materials using Maxwell's equations, highlighting the phenomena of polarisation and magnetisation. The chapter discussed the Drude-Lorentz model to predict the behaviour of dielectric materials and the Drude model for metallic properties. It further examined the concept of dispersion in optical materials and how different wavelengths of light refract differently through a lens. The chapter transitions to the design and optimisation of NIMs, focusing on manipulating their permittivity and permeability profiles to engineer desired optical properties. This involved the use of the Drude and Drude-Lorentz models to tailor the materials dispersive properties, highlighting the challenges in achieving a broadband negative refractive index. The chapter concludes with a demonstration of calculated materials using these models.

This chapter sets the stage by providing a thorough understanding of the fundamental physics and mathematical models underpinning the behaviour of NIMs. This foundational knowledge is crucial for delving into the design principles of singlet lenses using NIMs in the subsequent chapter.

5

THE FUNDAMENTALS OF NIM LENSES: FOCUSING ON REFRACTION

5.1 THIN LENS EQUATION

The thin lens equation is a key mathematical relationship used in geometric optics, particularly relevant to the design and understanding of optical systems using lenses.

The equation is a fundamental representation of the principles of lens optics. It is derived from the assumption that the lens is "thin", which refers to the thickness of zero. This assumption simplifies the complex wavefront interactions into a manageable set of geometric rules.

The thin spherical lens imaging equation provides the focal length (f) of a lens based on the radii of curvature of its surface and its material's refractive index. For a lens with radii of curvature R_1 and R_2 for the first and second surfaces, respectively, and the refractive index (n).

$$\frac{1}{f} = (n-1)\left(\frac{1}{R_1} - \frac{1}{R_2}\right)$$

The equation forms the basis of lens design, providing a relationship between the physical parameters of a lens and its optical power. It is important to note that the sign convention of radii of curvature is such that for a positive refractive index, R_1 is positive if the first surface is convex when viewed from the object side, and R_2 is negative if the second surface is concave when viewed from the object side.

The term n determines the contribution of the refractive index to the lens's power. When a lens made of negative refractive index ($n < 0$) is introduced, this term becomes negative, essentially inverting the lens's behaviour.

For a simple bi-convex lens, the focal length is normally positive as both R_1 and R_2 are positive. However, if the lens material possesses a negative refractive index, the focal length would turn negative, thereby behaving as a diverging lens instead of a converging lens.

In the context of the thin lens equation, a negative focal length would mean that a real object, which is usually placed on the side of the lens where light comes from, would form an image on the same side as the object. This is illustrated in figure 5.1, which demonstrates the actual fish location vs the perceived fish location when the waters index changes from positive to negative.

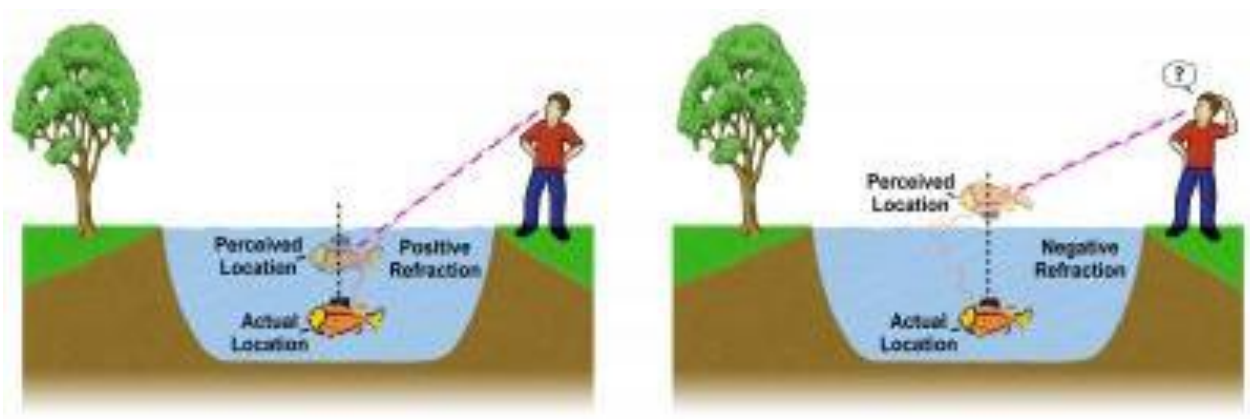

Figure 5.1. Illustration of how a fish is seen by an observer in (*right*) positive index material, and (*left*) negative index material.

The shape factor (α), or often referred to as the lens bending, defines the shape of the lens that impacts the performance of an optical system. It refers to the relative curvatures of the two surfaces of the lens, which can significantly influence the lens's aberration properties, in particular, spherical aberration, coma, and other higher-order aberrations. Designing a lens with the correct

shape factor can significantly improve its performance, minimizing aberrations, and providing better image quality.

$$\alpha = \frac{R_1 + R_2}{R_1 - R_2}$$

The negative refractive index causes the light to bend in the opposite direction as it would in a lens made of a material with a positive refractive index. This means that a flat (planar) lens made of a negative refractive index material can focus light, something that a flat lens made from a positive refractive index material cannot do.

This phenomenon can be attributed to the phase velocity of light being reversed in a negative index material. Hence, the wavefronts of the light are also reversed, causing the light to converge to a point after passing through a flat lens. This is contrary to the behaviour in a traditional lens where the lens must be curved to cause the light to converge.

The equations found in table 5.1 are deriving from the combination of the thin lens equation and the shape factor (α) to yield a defined equation for distinct α associated to the negative refractive index and focal position.

Table 5.1. Table of equations to calculate a defined lens bending according to the focal length and negative refractive index. An example has also been provided.

$\boldsymbol{\alpha}$	$\boldsymbol{R_1}$	$\boldsymbol{R_2}$	$\boldsymbol{R_1}$	$\boldsymbol{R_2}$
	Equations		Example: $f = 50mm$ & $n = -1.5$	
-3	$\frac{1}{2}f(n-1)$	$-(f - fn)$	-62.5	-125
-2	$\frac{2}{3}f(n-1)$	$2f(n-1)$	-83.3	-250
-1	$f(n-1)$	Inf	-125	Inf
0	$2f(n-1)$	$-2f(n-1)$	-250	250
1	Inf	$-f(n-1)$	Inf	125
2	$-2f(n-1)$	$-\frac{2}{3}f(n-1)$	250	83.3
3	$(f - fn)$	$-\frac{1}{2}f(n-1)$	125	62.5

Analysing the relationship between α and R_1, it can be determined that the correlation is a function of $1/x$:

$$R_1 = \frac{R_{1,max}}{\alpha - 1}$$

Therefore:

$$R_2 = \frac{(\alpha - 1)R_1}{(\alpha + 1)}$$

An example of the relationship between α and R_1 can be found in figure 5.3, and demonstrated that for any given lens shape factor, the associated lens radii can be determined.

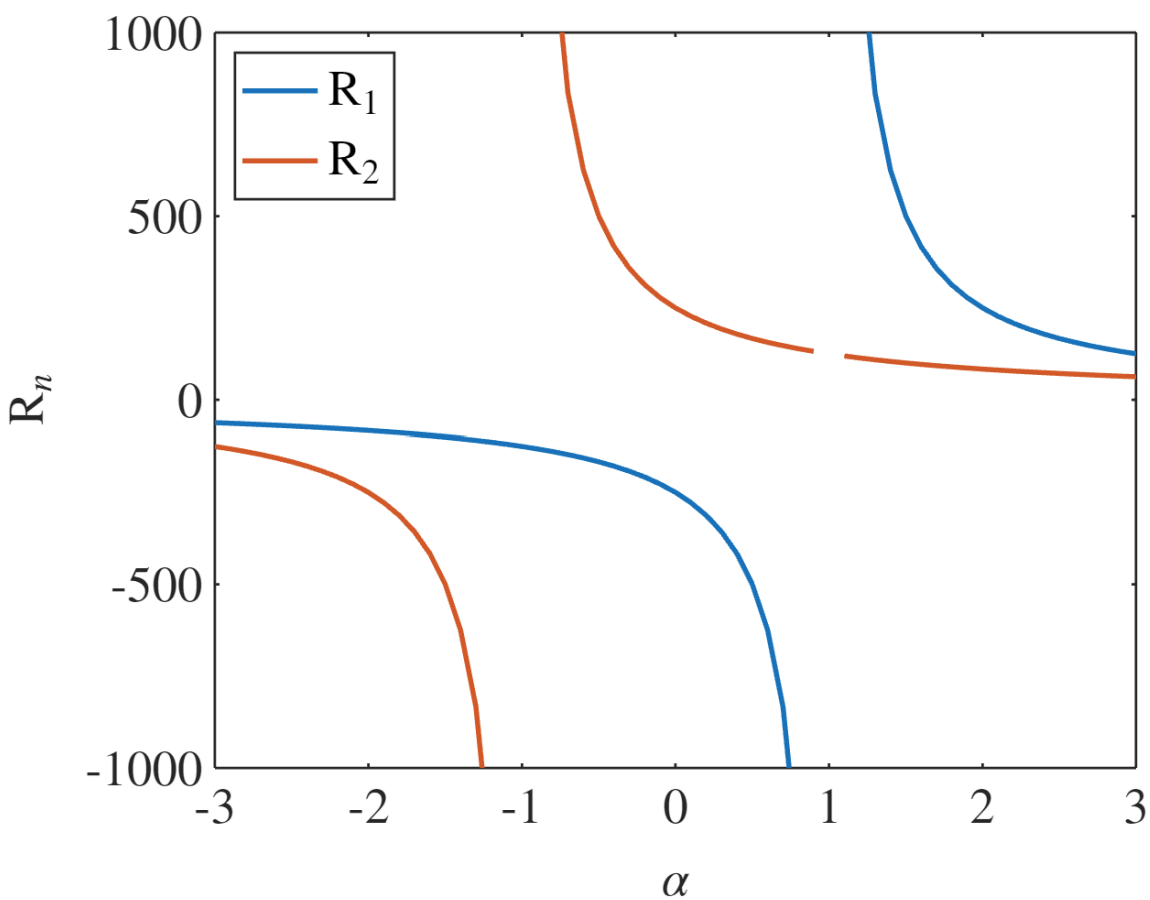

Figure 5.2. The associated radii for R_1 and R_2 for a given lens bending parameter (α), where $f = 50mm$ and $n = -1.5$.

5.2 THICK LENS EQUATION

The thick lens theory is a more generalised approach to lens optics compared to the thin lens approximation. In the thick lens model, the physical thickness of the lens is taken into account, which adds complexity to the analysis but also provides a more accurate representation of real-world lens behaviour.

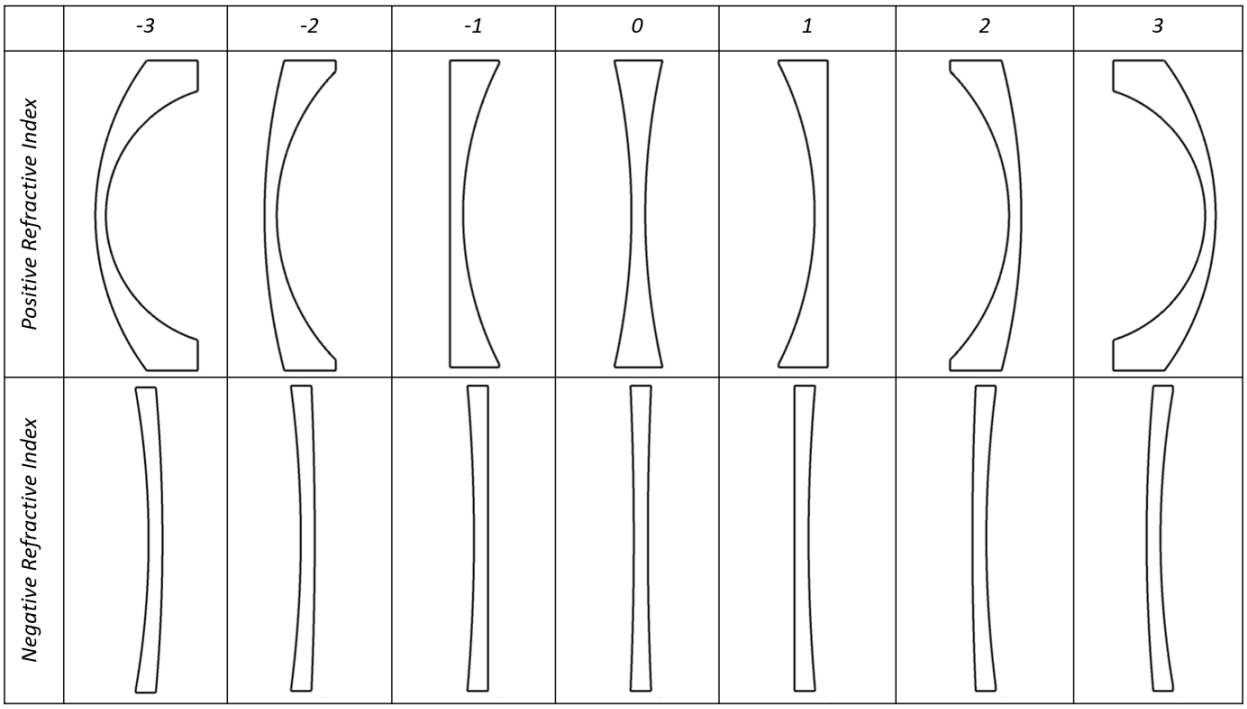

Figure 5.3. Comparison example of the lens curve for positive and negative refractive indices ($n = \pm 1.5$) with focal point of $f = 50mm$ and thickness of edge of $1mm$.

The lensmaker's formula for a thick lens (d), when derived using the principles of geometric optics, can be stated as:

$$\frac{1}{f} = (n-1)\left(\frac{1}{R_1} - \frac{1}{R_2} + \frac{(n-1)d}{nR_1R_2}\right)$$

From the above equation, the curvature of each surface (R_1 and R_2) contributes to the overall power of the lens, and thus to the position of the focal point. As the shape factor varies (by altering R_1 and/or R_2 while keeping the lens material and thickness constant), the lens power will

change. Table 5.2 demonstrates the effect of lens curvature on the focal distance between the two equations.

Table 5.2. Comparison of the thin and thick lens when $n = -1.5$ and $d = 2mm$.

α	R_1	R_2	*Thin Lens Focal Distance (mm)*	*Thick Lens Focal Distance (mm)*
-3	-62.5	-125	50	52.8169
-2	-83.3	-250	50	50.9896
-1	-125	Inf	50	50
0	-250	250	50	49.6689
1	Inf	125	50	50
2	250	83.3	50	50.9896
3	125	62.5	50	52.8169

For a positive lens with negative index (a lens that converges light), if $\alpha \geq 1$, the lens has a greater curve on the second surface, which means that it bends light more sharply on its exit than on entry. Due to the negative index, this results in a longer focal length, opposing the state of play presented with a positive refractive index.

The thickness of the lens also impacts the lens power. For a given shape factor and NIM, increasing the thickness of the lens will decrease the optical power, and thus increase the focal length.

5.3 Aberration

As presented in *Chapter 2*, optical aberrations are imperfections in the imaging process of an optical system, which leads to a deviation from the ideal image formation. Seidel aberrations are the group of five primary monochromatic aberrations and are fundamental in the study and design of optical systems. The equations are derived based on a paraxial approximation and third-order aberration theory.

Table 5.3. Simplified Siedel aberration equations.

Aberration	Equation
Spherical (S1)	$\sum \alpha_i (n-1) \left(\frac{h}{R_i}\right)^2$
Coma (S2)	$\sum \beta_i (n-1) \left(\frac{h}{R_i}\right)^3$
Astigmatism (S3)	$\sum \gamma_i (n-1) \left(\frac{h}{R_i}\right)^2 d_i$
Field Curvature (S4)	$\sum \delta_i (n-1) \left(\frac{h}{R_i}\right)^2 d_i^2$
Distortion (S5)	$\sum \epsilon_i (n-1) \left(\frac{h}{R_i}\right)^3 d_i$

The assessment of aberration within single lenses with varying refractive index and lens shape with a source object at infinite distance. The simulation setup can be found in Figure 5.4.

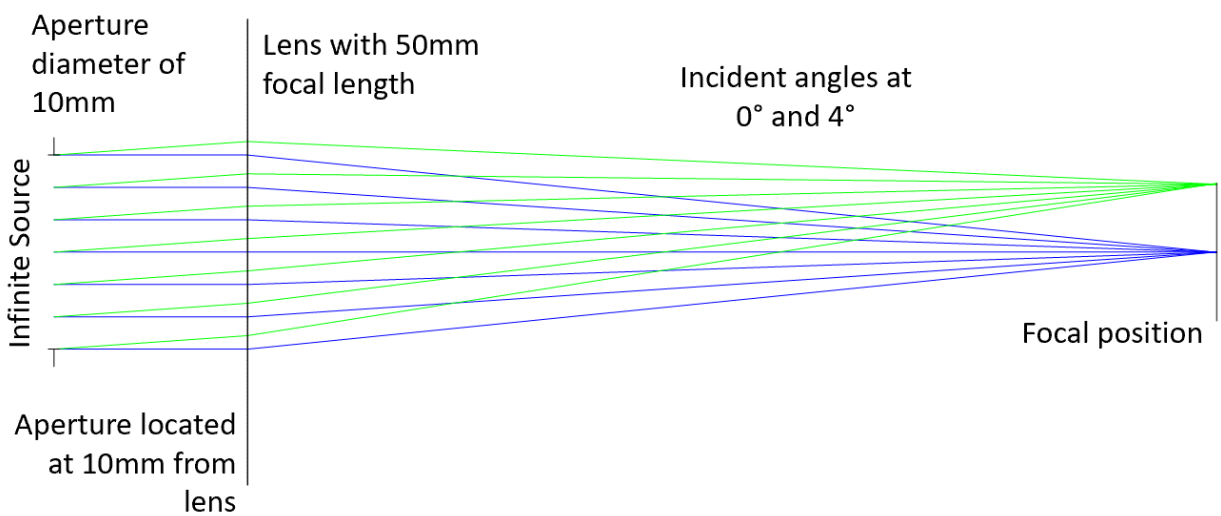

Figure 5.4. Simulation setup.

Figure 5.5 categorises the five types of aberration across different values of refractive index (n), assuming a lens with a shape factor set to zero, symmetric curvature radii. The refractive index varies from -2.5 to +2.5 in 0.25 increments. As the index varies from positive to negative, the way light is focus diametrically alters, thus affecting the aberrations differently.

Spherical aberration is more pronounced in lenses with a positive refractive index, suggesting that the convergence of light rays is less ideal at positive indices due to the more significant bending of light at the lens surface. As presented in Figure 5.2 and Figure 5.3, lenses with a positive index require greater curvature for a given lens shape compared to an opposing negative index of the absolute value. The requirement for lesser curved surface in negative index lenses is indicative of an alternate focusing mechanism inherent to the material itself, as found in Figure 1.3b and discussed by Pendry.

Coma and astigmatism appear less sensitive to the sign change of the refractive index, maintaining a relatively low magnitude throughout these singlet examples. This suggests that the off-axis aberrations are not as strongly influenced by the sign of the refractive index as by the geometry of the lens or position of the object.

The field curvature and distortion aberrations exhibit a relatively consistent low magnitude across the range. The consistent level of field curvature suggests that the image plane curvature is not drastically affected by the variation of index. Similarly, distortion levels indicate that the geometric integrity of the image is preserved across different materials, which might be particularly relevant in systems where the accuracy of image geometry is critical.

Figure 5.6 presents ray tracing diagrams for two lenses with indices of ±1.25, both with a lens shape set to zero. The root mean square (RMS) error, measured in radians, quantifies the deviation of the rays from the ideal focus, where a lower RMS indicates a more precise focus of the rays through the lens.

For the lens with n = -1.25, the RMS value is relatively low at 21.049 radians, suggesting that the rays are converging more closely to the ideal point, as evident from the corresponding spot diagram on the right, which is zoomed in by a factor of 5.

Conversely, the lens with n = +1.25 shows a significantly higher RMS value of 139.551 radians, indicating a substantial deviation from the ideal focus and a less precise convergence of light rays. The corresponding spot diagram, displayed at a standard zoom of 1x, reveals a larger dispersion of focal points, implying a lower optical quality and higher aberration. The spread of the spot pattern is indicative of substantial spherical aberration.

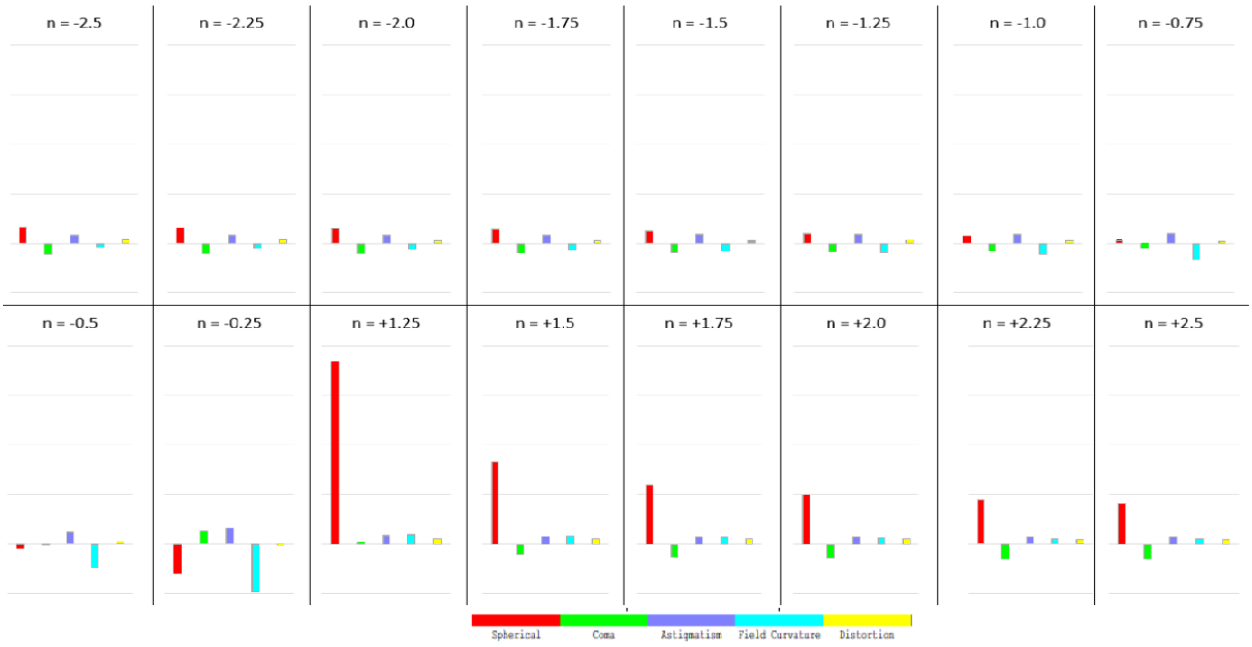

Figure 5.5. Aberrations for varying refractive index with lens shape factor set to zero (symmetric curvature radii) for set up found in Figure 5.4. The grid lines are spaced at 0.01mm. Spherical (red), come (green), astigmatism (purple), field curvature (blue), and distortion (yellow).

The comparison between the two lenses is stark; despite the same absolute value of the refractive index, the positive index lens suffers from significantly higher aberration, as evidenced by the RMS and the spread in the spot diagram. This suggests that materials with negative refractive indices could potentially be harnessed to design lenses with unique focusing properties, possibly enabling more compact lens systems without the need for complex aspheric designs to correct for aberrations.

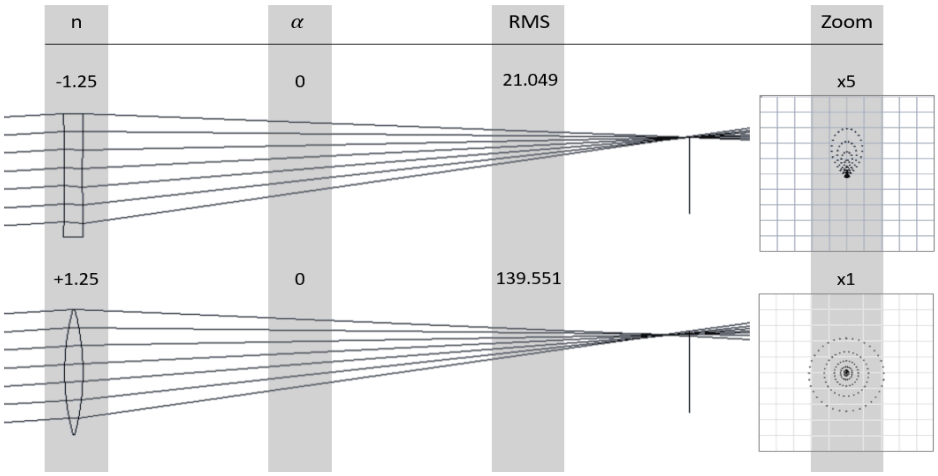

Figure 5.6. Ray traced diagrams comparing index variation of ±1.25 with a lens shape factor of zero. The RMS is measured in radians. The spot diagram zooms are shown to the *right*. Lens thickness is 1.5 mm. The field axis is at 4°.

Figure 5.7 provides a series of three-dimensional plots that illustrate the relationship between the primary monochromatic aberrations and two key optical parameters, refractive index and lens curvature. The insights provided from the data are pivotal for the development of optical systems, informing decisions on material choice and lens geometry to minimize aberrations for improved image quality.

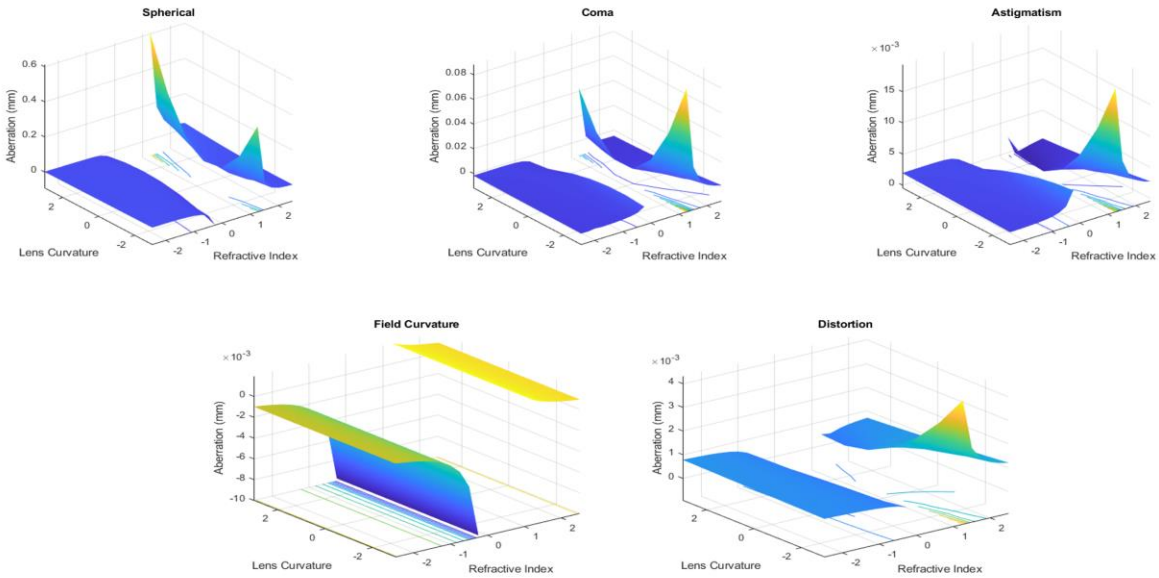

Figure 5.7. 3D plots of the primary monochromatic aberrations showing the effects of refractive index and lens curvature combined, with 2D isometric projections highlighting the extremes.

Figure 5.8 is a comprehensive representation of the impact of lens shape factor (α) on the performance of optical lenses with both positive and negative refractive indices (n). The diagrams show ray traces for three different lens shapes at each refractive index, with shape factors of -2, 0, and +2.

For lenses of positive refractive index, it can be observed that the RMS error is significantly affected by the lens shape factor. The lens with a shape factor of -2 demonstrates a considerable RMS value of 169.060, which suggests substantial deviation from the ideal focus, possibly due to increased spherical aberration as indicated in the corresponding Seidel plot. When the shape factor is zero, indicating a symmetrical lens, the RMS error decreases to 70.369, implying better focusing performance. However, for the lens with a shape factor of +2, the RMS error escalates to 341.320, indicating a dramatic decrease in optical performance, which is likely due to the exacerbated higher-order aberrations.

Comparatively, lenses with a negative refractive index demonstrate a markedly different trend. The RMS error is consistently lower across all shape factors, with the highest RMS being 25.960 for the shape factor of -2 and the lowest being 19.162 for the shape factor of +2. This suggests that lenses with a negative refractive index are less sensitive to the shape factor in terms of aberrations, potentially offering a more robust optical design space.

The Seidel aberration plots provide additional insight into the specific aberrations contributing to the RMS error. For positive index lenses, there is a prominent presence of all five Seidel aberrations, particularly spherical aberration and coma. In contrast, the negative index lenses show a significant reduction in these aberrations, with notably lower levels of spherical and coma aberrations. This improved performance in negative index lenses is quite remarkable and

suggests that such materials could be advantageous in optical systems requiring high precision focusing.

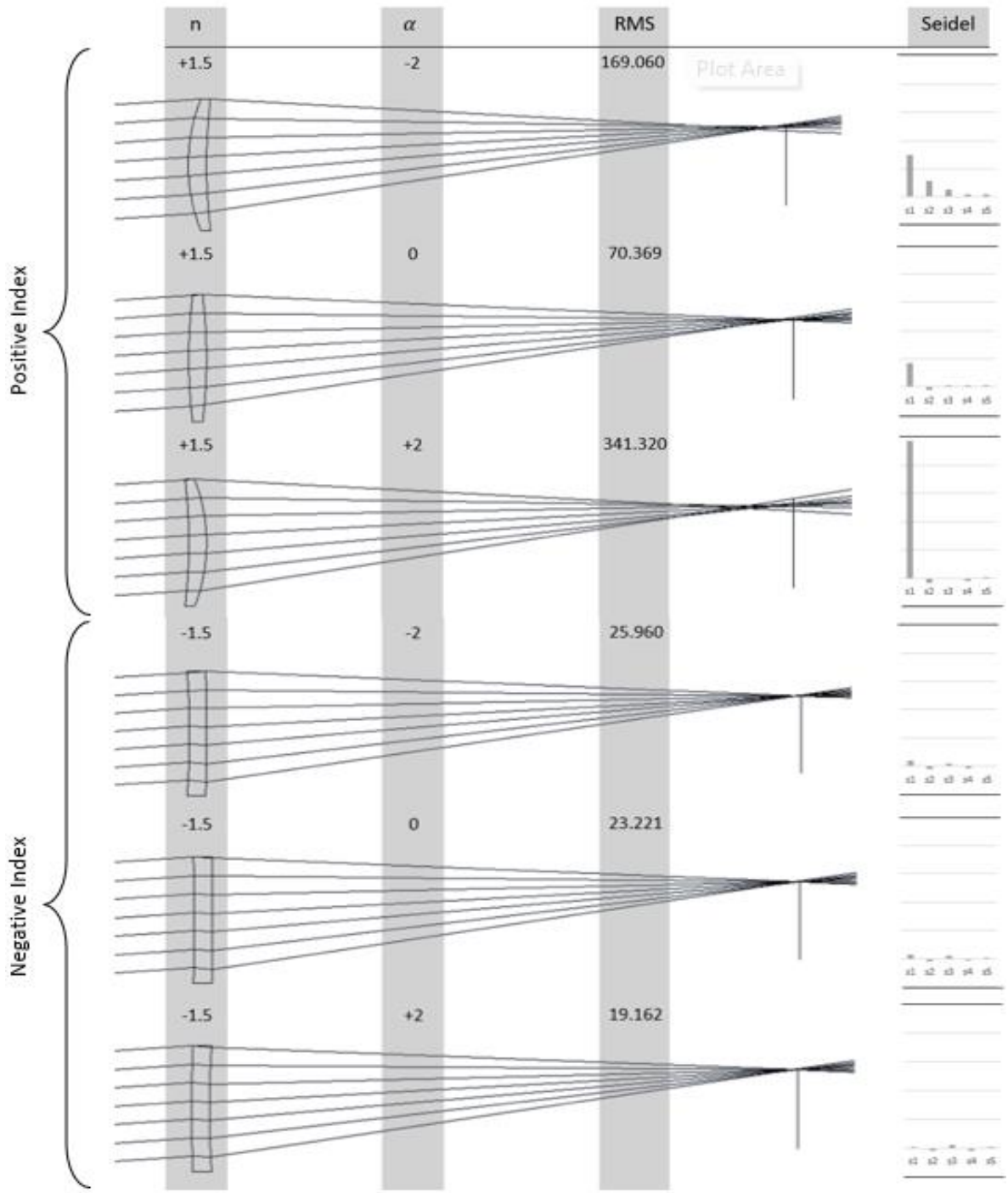

Figure 5.8. Ray traced diagrams show the effects of lens shape with positive and negative refractive index. The Seidel aberrations demonstrate the improved comparative performance for negative index lenses. The grid lines are spaced at 0.02mm. aberrations are indicated as spherical (s1), coma (s2), astigmatism (s3), field curvature (s4), and distortion (s5).

5.4 CHAPTER SUMMARY

The chapter meticulously explores the principles and applications of negative refractive index materials (NIMs) in optical lenses, focusing on the thin and thick lens equations. It demonstrates how NIMs alter traditional lens behaviour, enabling the design of lenses that can, intriguingly, focus light with flat or slight spherical curves, effectively reducing optical aberrations. This breakthrough presents a shift in optical design, offering new avenues for developing more compact and efficient optical systems without the need for complex geometries traditionally used to correct aberrations.

Following this foundational work, the subsequent chapter aims to apply these principles to the design of an optical system within the context of Industry 4.0, focusing on machine vision. It will explore the integration of NIM-based lenses into optical systems that require high precision and flexibility, addressing the challenges of designing such systems and the potential advantages NIM materials offer in terms of system compactness, efficiency, and aberration correction. This discussion will be pivotal for advancing optical system design, particularly in applications demanding high resolution and accuracy in automated, real-time environments.

6

OPTICAL DESIGN: AN INDUSTRY 4.0 MACHINE VISION APPLICATION

6.1 INTRODUCTION TO OPTICS IN 3D IMAGING

The introduction of industry 4.0 has heralded a transformative era in manufacturing, characterised by automation, data exchange, and advanced technologies. Central to this revolution is the requirement for optical systems, acting as the digital eyes for monitoring and detection within the advanced manufacturing process. A critical component in machine vision is 3D imaging.

Optical design in 3D imaging encompasses a myriad of challenges, primarily revolving around the precise capture and interpretation of spatial information. Key challenges include managing aberrations in lens system, ensuring accuracy in depth perception, and optimising illumination for clear imaging. As these challenges are navigated, the effectiveness of 3D imaging in industrial applications is significantly influenced, marking its criticality in the ongoing evolution of Industry 4.0.

6.2 METHODS FOR NON-CONTACT 3D METROLOGY IN I4.0

Non-contact 3D metrology encompasses a variety of techniques essential for precise and efficient dimensional measurements in Industry 4.0 applications. Key methods include Time of

Flight, which measures the time taken by a light pulse to travel to an object and back; Stereo Vision, using two or more cameras to simulate human binocular vision; Structured Light Projection, projecting a known light pattern onto an object and analysing the deformation for 3D reconstruction; and Laser triangulation, projecting a laser line or dot onto an object where a camera with known positions can capture the image of the laser as it appears on the objects.

6.3 Challenges in Optical Design for 3D Imaging

The Scheimpflug Condition, a fundamental principle derived from geometric optics, necessitates precise alignment of the lens's tilt relative to the image sensor. This alignment ensures uniform focus across various object depths, particularly in wide-field systems. Unlike conventional imaging where the object plane and sensor plane are parallel, applying a tilt to these planes facilitates depth of focus within a single optical system.

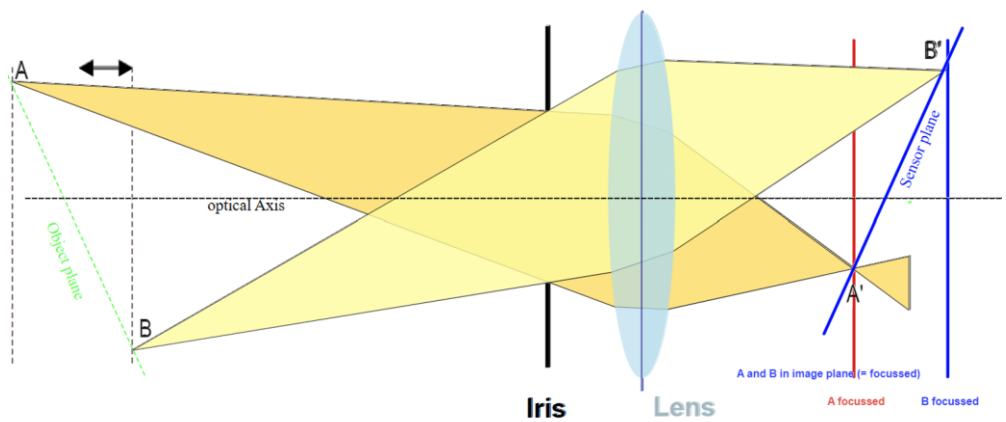

Figure 6.1. Schematic demonstrating different object distances that have different image distances. Scheimpflug's idea involves tilting the sensor plane to perceive the depth of focus.

6.4 Optimisation Techniques

In optical design for 3D imaging, several strategies are employed to overcome challenges and achieve a balance between resolution, depth range, and lens complexity. Adjusting the triangulation angle is a key technique. This involves altering the angle between the camera and the illumination source to optimise depth accuracy and field of view.

Addressing the Scheimpflug condition requires careful lens tilting and aperture adjustments to ensure uniform focus across the imaging field.

Higher resolution often requires more complex lens systems, which can increase cost and size. Conversely, simpler lenses might limit resolution but offer reduced costs.

The use of NIMs in a complex optical system like this, could significantly mitigate the adverse effects of aberrations likes spherical and chromatic aberration. This is because NIMs can refract light in ways that counteract the distortion typically introduced by conventional lenses. Therefore, allowing for a broadband optical solution, opposing a single laser wavelength illumination solution that might be used with conventional positive index lenses. The benefit of a broadband approach compared to laser methods lies in its capability for colour observations.

6.5 Noteworthy Benefits to the NIM Solution Over the PIM Solution

Scheimpflug systems with conventional lenses, using positive index materials (PIMs), are documented to be effective solutions for laser triangulation 3D imaging. Govier (2019) effectively discusses how to “handle” the optical design challenges in 3D imaging using laser triangulation which could be an effective solution for many i4.0 applications but has some significant limitations.

Utilising the principles presented in the previous two chapters, replacing PIMs with NIMs should improve the systems spherical and chromatic aberrations, enabling for a full colour system in place of a single mono-colour from the laser source. This will improve the 3D imaging system notably. The key comparisons are presented in Table 6.1.

Table 6.1. Comparison of broadband solution using NIMs compared with the traditional laser triangulation method.

Subject of consideration	Laser Solution	Broadband Solution
Speckle Noise	Lasers, due to their coherent nature, often produce speckle noise in images. Speckle noise is a granular interference that degrades image quality, making it challenging to discern fine details.	Broadband sources, being incoherent, significantly reduce or eliminate speckle noise. This results in clearer images with higher fidelity.
Colour Rendering	Lasers typically emit light at a single wavelength, limiting the colour range in the resulting images. This makes it difficult to accurately represent or distinguish between colours in the imaged objects, reducing the effectiveness of the imaging system in tasks requiring colour discrimination.	Broadband sources, such as halogen or LED lights, cover a wide spectrum of wavelengths, enabling the capture of images with full colour rendition. This is essential in industries where colour accuracy is paramount.
Versatility and Compatibility	Laser systems often require precise alignment and safety measures, which can limit their flexibility and application scope. Their monochromatic nature also makes them less compatible with applications requiring multispectral or hyperspectral imaging.	Broadband sources are more versatile and can be easily integrated into a wide range of imaging systems. They are compatible with various detectors and cameras, allowing for multispectral and hyperspectral imaging applications.
Depth of Field	The coherence of laser light can lead to limitations in the depth of field of an imaging system, especially in high-resolution applications. This may necessitate additional adjustments or compromises in system design.	Broadband solutions can provide a larger depth of field, making it easier to image objects at different distances from the lens without losing focus.
Safety and Comfort	Lasers, especially those of higher power, pose safety risks to operators and subjects, including potential eye damage. Safety precautions and protective gear are necessary, which can complicate and slow down workflows.	Broadband sources generally present fewer safety concerns and are more comfortable for both operators and subjects enhancing the usability and accessibility of imaging systems.

Transitioning from a laser imaging system to a broadband imaging system can be particular benefits to i4.0 by enhancing automation, quality control, and data analytics capabilities. Table 6.2 presents some of the key advantages.

Table 6.2. Key advantages for i4.0 applications.

Advantage	**Reasoning**
Higher Speed and Efficiency	Broadband optical imaging systems can capture high-resolution images at a faster rate compared to laser triangulation systems. This is crucial for real-time monitoring and control in automated manufacturing processes, enabling quicker decision-making and adjustments.
Greater Versatility	Broadband optical systems can capture a wide range of wavelengths, providing flexibility in imaging different types of materials and surfaces. This versatility is beneficial in diverse industrial applications, from quality control in manufacturing to inspection in agriculture, where different materials and conditions are encountered.
Enhanced Image Quality and Detail	The ability to capture images across a broad spectrum can result in higher quality images with more detail. This is particularly important for applications requiring precise measurements and detailed inspections, as it allows for more accurate analysis and defect detection.
Cost-Effectiveness	Broadband optical imaging systems can be more cost-effective in the long run due to their durability and lower maintenance requirements. Unlike laser systems that may require frequent calibration and can suffer from laser diode degradation, broadband systems can offer longer service life with less intensive maintenance, reducing total cost of ownership.
Integration and Scalability	Broadband optical imaging systems can be more easily integrated into existing Industry 4.0 infrastructures, supporting IoT (Internet of Things) connectivity and data analysis platforms. This integration capability allows for scalable solutions that can grow with the needs of the industry, facilitating the collection, analysis, and utilisation of imaging data across various applications.

While laser triangulation systems have been widely used for 3D imaging due to their precision and reliability, a broadband optical imaging systems would offer a range of benefits that align well with the needs of Industry 4.0.

6.6 Optical Solution of Broadband White Light System using NIM Lenses

Figure 6.2 offers a comparison design solution for the laser triangulation system with PIMs and a broadband 3D imaging system with NIMs. Both designs facilitate the same number of elements with a similar system length and F-number, *a measurement of light-gathering ability of an optical system.* Both designs also facilitate a Scheimpflug condition for positional focal planes to achieve three-dimensional imaging.

The negative refractive index materials used in the design solution found in Figure 6.2b are not optimised for the solutions and remain generalised to the parameters discussed in Table 4.1 and presented in Figure 4.7.

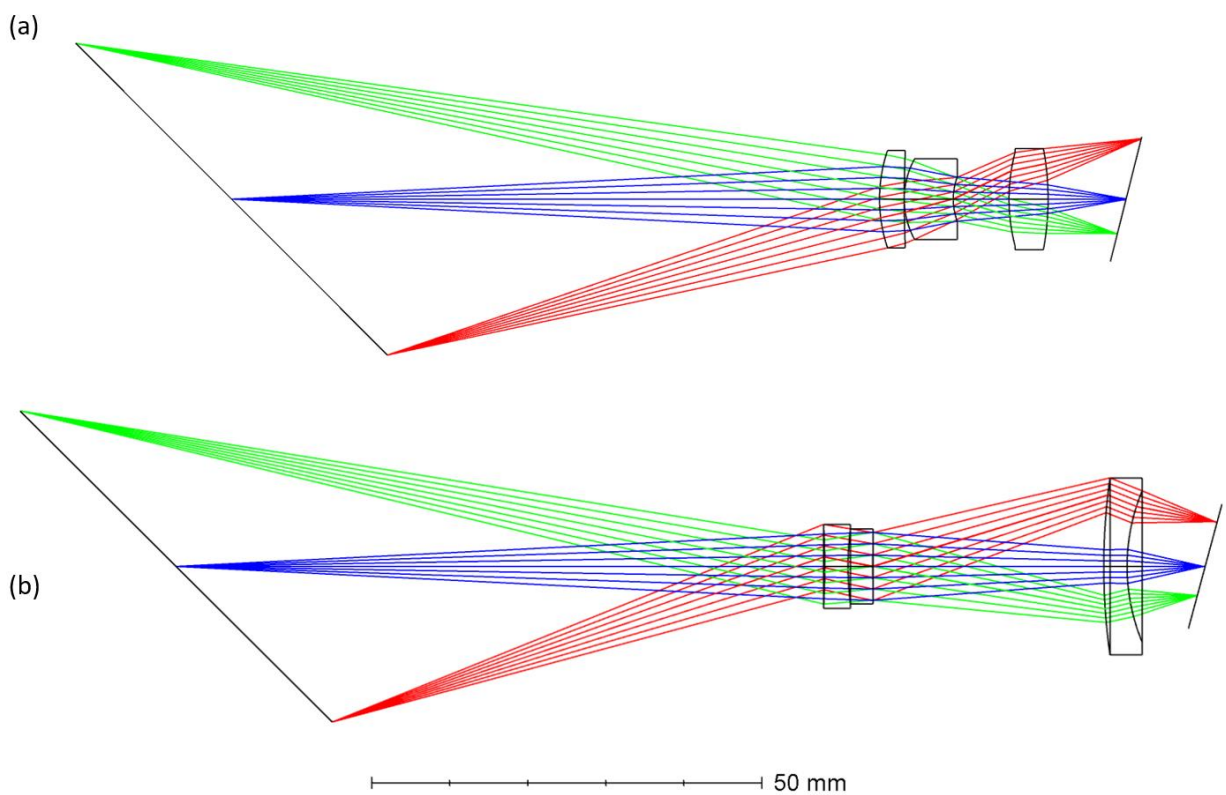

Figure 6.2. Optical design of 3D Industry 4.0 imaging system with (a) positive index materials and (b) negative index materials. The ray colours differ to highlight the varying fields, not the wavelength of light.

Table 6.3 provides an overview of the design parameters that have been inputted into Zemax® optical design software. The parameters also showcase the similarities between the two systems, demonstrating the advantages arise from the material selection oppose to any design choices such as aspherical surfaces.

Table 6.3. The design prescription of the two designs.

Surface Number	Surface Type	Radius (mm)	Thickness (mm)	Material	Clear Semi-Diameter (mm)	Tilt (Y-Tangent)
PIM						
0	Objective – Tilt	-	83.060	Air	20	-1.000
1	Spherical	19.614	3.163	SK16	6.249	-
2	Spherical	138.600	-8.304e-4	-	5.662	-
3	Spherical	10.730	6.288	F2	5.164	-
4	Spherical – Stop	8.121	7.148	-	2.839	-
5	Spherical	26.623	5.006	SK16	6.008	-
6	Spherical	-35.431	9.999	-	6.498	-
7	Image - Tilt	-	-	Air	7.816	0.251
NIM						
0	Objective – Tilt	-	83.060	Air	28.284	-1.000
1	Spherical	-99.598	2.997	NIM-A	5.879	-
2	Spherical	36.749	-8.986	-	5.052	-
3	Spherical	36.828	3.178	NIM-B	5.502	-
4	Spherical – Stop	357.117	29.582	-	4.399	-
5	Spherical	82.303	2.986	NIM-A	14.921	-
6	Spherical	25.514	9.999	-	12.222	-
7	Image - Tilt	-	-	Air	8.031	0.269

Figure 6.3 show the relationship between the focal shift (in micrometres) and the wavelength (also in micrometres) for both the PIM and NIM designs. The focal shift refers to the change in the position of the focus of a lens system when the wavelength of light changes. The PIM solution is typical for a laser system as chromatic aberrations are not a concern as only the focal length at the laser wavelength is considered.

The laser PIM solution is monotonically increasing, meaning as the wavelength of light increases, the focal shift also increases. This is characteristic of normal dispersion in positive index materials (despite efforts to correct with crown and flint materials), where longer wavelengths (red light) are less "bent" than shorter wavelengths (blue light), causing red light to focus further away from the lens.

The insert of Figure 6.3 shows a magnified view of the NIM solution curve, indicating that the focal shift values for NIM are much smaller in the range of interest, meaning that the NIM design is an excellent broadband imaging solution as it effectively eliminates the chromatic aberration.

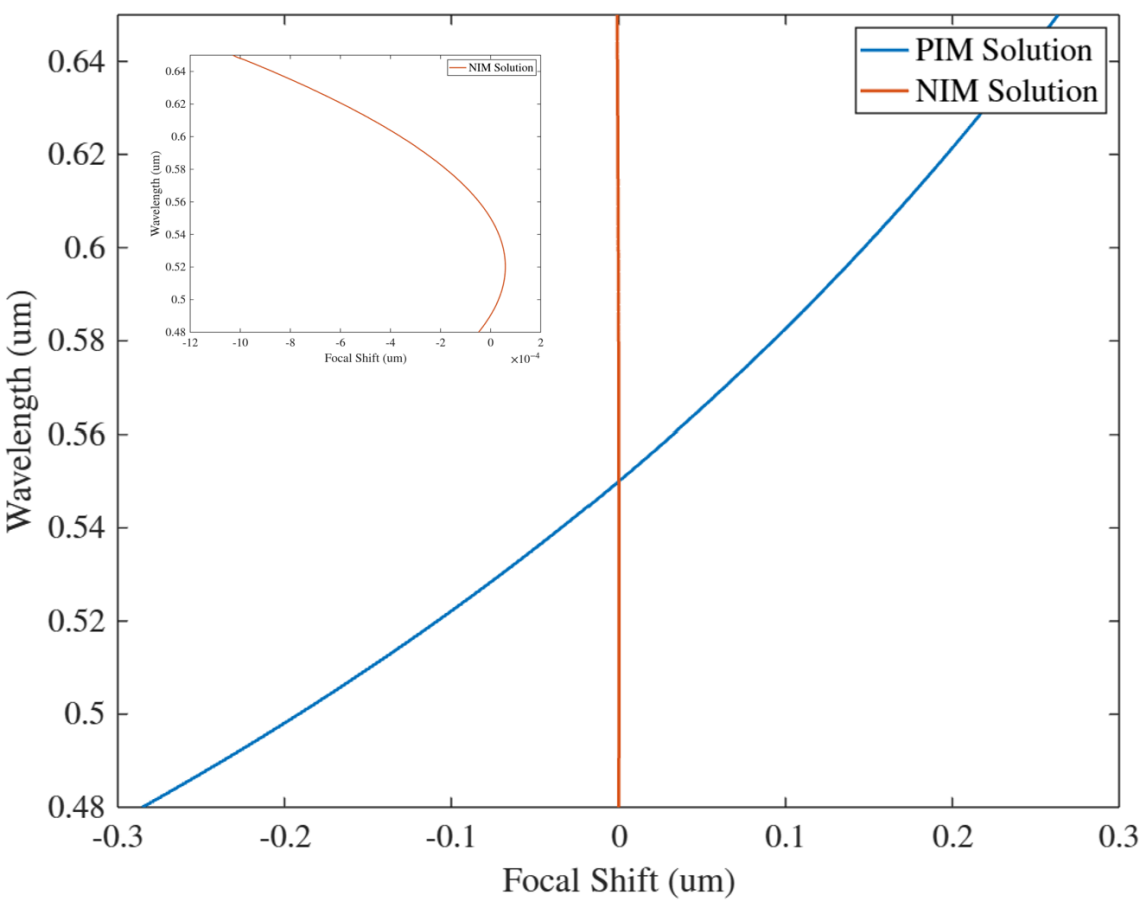

Figure 6.3. A comparative chromatic focal shift evaluation. *Insert* showing the extent of the NIM focal shift.

This chromatic aberration can also be viewed in the simulated image, where Figure 6.4a clearly demonstrates colour variation across the entire field, meaning that different wavelengths are locally focused on the imaging plane, and where Figure 6.4b produces a clean white colouration at the image plane demonstrating that all wavelengths are focused on the imaging plane.

Figure 6.4 shows a simulated mesh of the two designs presented in Figure 6.2. Both cases demonstrate the titled image plane. The grid pattern for the PIM laser solution appears to be distorted in a manner consistent with conventional lens behaviours. The lines of the grid that are closer to the centre appear less distorted, while those towards the edges display more pronounced curvature, with a maximum distortion of 36.8261%. The grid for the NIM solution shows a different type of distortion. While still curved, the lines do not exhibit the same degree of bending towards the edges as seen in Figure 6.4a, with a maximum distortion of 25.5071%.

It should also be noted that that edge focusing on the NIM solution is slightly worse than the PIM solution but the central focusing is quantifiably better.

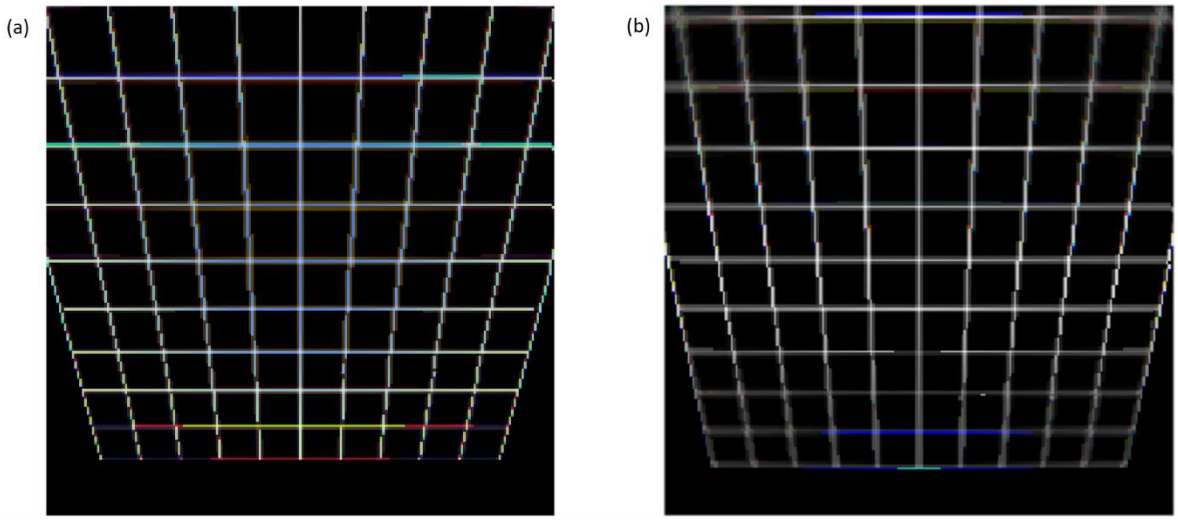

Figure 6.4. Simulated image through the optical systems of (a) positive index design, and (b) negative index design.

Figure 6.5 represents a comparative aberration evaluation between the designs presented in Figure 6.2. Overall, the NIM solution offers significant improvements in some aberration, particularly spherical and chromatic longitudinal aberration (as predicted from *Chapter 5*'s results), while potentially increasing others like astigmatism and introducing negative field curvature. The evaluation of these aberrations is critical in optical system design, as they affect the image quality. The ideal lens design would minimise all types of aberrations, but in practice, trade-offs often need to be made depending on the specific application and constraints of the system. The negative index materials show promise, but the increased astigmatism and field curvature suggest that there are still challenges to be addressed in the use of these materials for optical systems. A summary comparative evaluation can be found in Table 6.4.

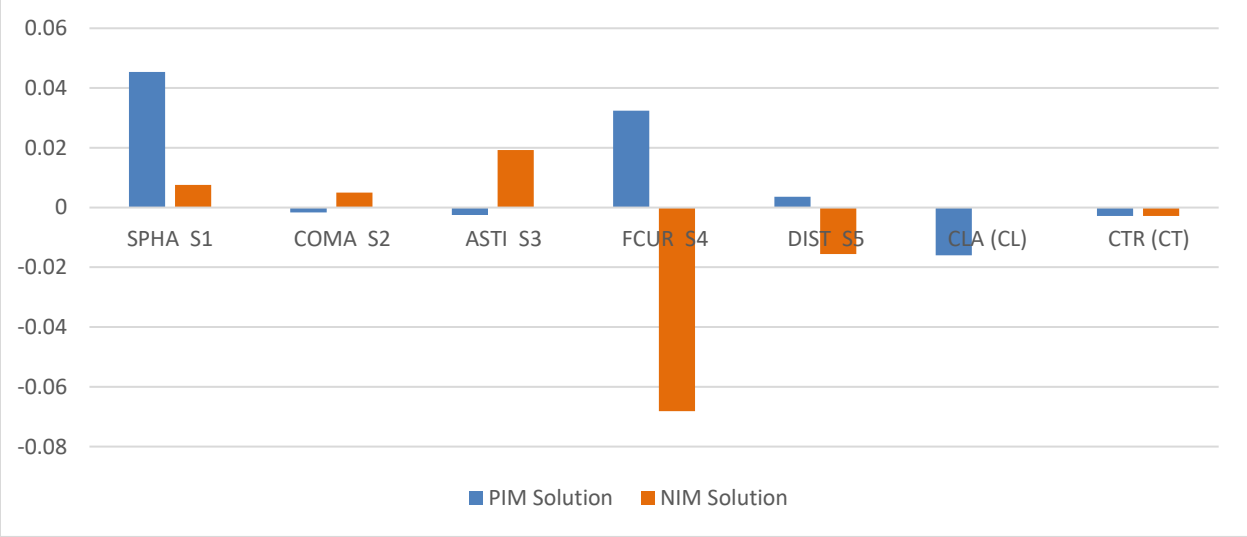

Figure 6.5. A comparative aberration evaluation of (a) positive index design, and (b) negative index design.

Table 6.4. Comparative summary of the aberrations found in both Figure 6.2 designs.

Aberration	PIM Design	NIM Design
Spherical (SPHA S1)	A significant amount of spherical aberration (0.045417), which is typical for positive index lenses where rays farther from the optical axis are refracted more strongly.	A much lower spherical aberration (0.00757), suggesting that negative index materials might correct for this aberration better than PIM, as discussed in *Chapter 5*.
Comatic (COMA S2)	Negative coma (-0.001642), which might indicate that the outer rays are focused slightly closer to the lens than the paraxial rays.	Positive coma (0.004975), meaning that the outer rays are focused slightly further from the lens than the paraxial rays.
Astigmatism (ASTI S3)	A small negative astigmatism (-0.002531), which could mean the vertical and horizontal foci are not at the same distance from the lens.	A higher positive astigmatism (0.019252), which could cause more pronounced image blur at different planes.
Field Curvature (FCUR S4)	A positive field curvature (0.032448), indicative of a curved image plane, which can cause the edges of the image to appear out of focus when the centre is in focus.	A negative field curvature (-0.068097), suggesting a corrective effect but might introduce a different type of defocus towards the edges.
Distortion (DIST S5)	A slight positive distortion (0.003641), which indicates pincushion distortion where lines bow inwards.	A moderate negative distortion (-0.01555), which indicates barrel distortion where lines bow outwards.
Chromatic Longitudinal (CLA (CL))	A negative chromatic longitudinal aberration (-0.016034), which might mean that different wavelengths focus at slightly different distances.	An almost neutral chromatic longitudinal aberration (0.000048), suggesting a significant reduction in chromatic aberration compared to PIM.
Chromatic Transverse (CTR (CT))	Both PIM (-0.002858) and NIM (-0.002808) have similar small negative values for chromatic transverse aberration, indicating that there might be minor colour fringing at the image periphery.	

6.8 CHAPTER SUMMARY

The chapter investigated the utilisation of NIMs for enhancing the optical design of a 3D imaging system within an industry 4.0 setting. The NIM solution reveals a significant advancement in reducing spherical aberration and virtually eliminating chromatic aberration, when compared to traditional PIM designs.

While the NIM design maintains or increased other aberrations relative to the PIM configuration there exists a potential for further aberration mitigation through the strategic design of materials with negative refractive indices, *discussed in Chapter 4*, tailored to address specific aberrations.

A critical advantage of the NIM optical design over the PIM optical design is it its capacity to support broadband imaging capabilities, in contrast to the PIM's limitation to single-laser wavelength operations. Although traditional PIM systems offer avenues for improvement, such enhancements would necessitate a complex redesign, incorporating a greater number of lens elements, thereby increasing the system's complexity.

This chapter underlines the transformative potential of NIMs in optical design, suggesting a potential theoretical paradigm shift towards more versatile and efficient imaging solutions by specifically designing the negative refractive index material properties.

7

CONCLUSION: CONVERGING THE FUTURE

A review of the novel developments discussed in this thesis, include:

- The utilisation of the Drude and Drude-Lorentz equations to tailor the negative refractive index and dispersion properties for a given artificial material over a broadband wavelength range.
- The study of negative refractive index and its effect on lens shape and their resulting aberrations, demonstrating the potential to significantly reduce aberrations using NIMs, particularly spherical and chromatic aberration.
- Applied theoretically designed NIMs to a 3D imaging system for applications in i4.0 demonstrating improved optical performance compared with conventional 3D imaging systems with PIMs.

7.1 CONCLUSION

Do the benefits of incorporating generalised NIM lenses into optical systems through SWAP-C optimisation exist, and if so, how can they drive optical innovation?

The fundamental premise behind incorporating NIMs into optical designs lies in their unique ability to manipulate light in ways that traditional PIMs cannot. NIMs exhibit negative refraction, allowing for the design of lenses and optical components that can overcome limitations

such as chromatic aberration, spherical aberration, and diffraction limits which are inherent in conventional optical materials (Smith et al., 2004; Veselago, 1968).

The first chapter introduces the concept of SWAP-C optimisation as a critical framework for advancing optical design within the constraints of modern technological applications. It suggests that by integrating NIMs into optical systems, designers can achieve superior performance metrics while adhering to stringent size, weight, and power constraints, whilst costing remains unanswered. This is particularly relevant in applications such as telecommunications, imaging systems, and sensors where these factors are critical to the deployment and operational efficiency of the technology.

In Chapter 4, a detailed examination of the mathematical characterisation of light's interaction with materials, particularly focusing on polarisation and magnetisation, sets the stage for understanding the unique properties of NIMs. The chapter discusses the Drude-Lorentz model's application to predict dielectric materials' behaviour and the Drude model for metallic properties. This lays the groundwork for exploring the challenges and strategies in designing NIMs with desirable dispersive properties by manipulating their permittivity and permeability. These discussions are critical for advancing the design and optimisation of NIMs, highlighting the potential for engineered materials to achieve broadband negative refractive indices, a cornerstone for the next generation of optical innovations.

Subsequent chapters delve into the technical advantages of NIMs in optical systems. For instance, Chapter 5 highlights the ability of NIM-based lenses to significantly reduce spherical and chromatic aberrations. This improvement is attributed to the anomalous dispersion properties of NIMs, which can be engineered to achieve a flat lens design, thereby simplifying optical systems and reducing the number of necessary components (Pendry, 2000). The reduction in components

not only impacts the system's size and weight but also contributes to cost reductions in manufacturing and maintenance.

Furthermore, the use of NIMs in optical systems is shown to enhance imaging capabilities, as exampled in 3D imaging applications as discussed in Chapters 6. NIMs enable a broader depth of field and improved image quality across a wider range of wavelengths compared to traditional PIM-based systems. This broadens the applicability of optical systems in diverse fields such as but not limited to biomedical imaging, where detailed, high-resolution images are crucial for diagnostics and research (Zhang et al., 2008).

Moreover, the SWAP-C optimisation framework, when applied with NIMs, facilitates the development of more compact, lightweight, and power-efficient optical devices. These devices exhibit enhanced performance characteristics, making them highly desirable for a wide array of applications. The incorporation of NIMs into optical systems thus represents a significant step forward in the field of optics, offering the potential to revolutionise how light is manipulated and utilised across various technological domains.

The academic literature supports these claims, with numerous studies highlighting the theoretical and practical benefits of NIMs in overcoming traditional optical limitations (Leonhardt, 2006; Ramakrishna, 2005). The potential for NIMs to drive innovation in optical design is immense, given their unique properties and the growing demand for more efficient, compact, and cost-effective optical solutions. They are poised to catalyse a paradigm shift in optical technologies, heralding advancements previously relegated to the realm of science fiction. NIMs, with their unprecedented control over light, could enable the development of hyper-resolution optical imaging systems, penetrating the barriers of the diffraction limit and opening new vistas in biomedical research and nanoscale engineering (Pendry, 2000). Beyond imaging, NIMs promise

the materialisation of invisibility cloaks, leveraging their unique refractive properties to bend light around objects, a concept that could transform stealth technology and privacy measures (Leonhardt, 2006). Additionally, the integration of NIMs into photonic circuits could dramatically miniaturise optical components, leading to ultra-compact, highly efficient devices for telecommunications, computing, and sensing applications, fundamentally redefining the architecture of future technologies (Zhang et al., 2008). As research progresses, these visionary applications of NIMs are not only conceivable but increasingly attainable, marking the dawn of an exhilarating chapter in optical innovation.

In conclusion, the benefits of incorporating generalised NIM lenses into optical systems through SWAP-C optimisation are evident and multifaceted. They offer a promising avenue for overcoming traditional optical limitations, enhancing imaging capabilities, and meeting the stringent requirements of modern technological applications. As research and development in this area continue to advance, it is likely that the use of NIMs in optical systems will play a pivotal role in driving innovation across various fields. The integration of NIMs, guided by the principles of SWAP-C optimisation, thus represents a significant leap forward in the pursuit of more versatile, efficient, and impactful optical technologies.

7.3 Suggestions for Future Work

The next stage of this work would be to expand the mathematical investigation to include the imaginary components that describes a material absorbing properties and examine how a complex negative refractive index influences aberration. Beyond this, investigations into the artificial atoms and their base material configurations also require a thorough scientific investigation to ascertain the feasibility of manufacturing the desired materials.

REFERENCES

Author, Imaginary. 2011. *This Is an Example Source.* Boise: Boise State University Publishing.

Doe, John. 1903. *Imaginary Text.* London: Red Herring Press.